NGU Report 2011.021

Potential of rare earth element and Zr-, Be-, U-, Th-, (W-) mineralisations in central and northern Nordland – Part 2

NGU
Norges geologiske undersøkelse
Geological Survey of Norway

Geological Survey of Norway
NO-7441 Trondheim, Norway
Tel.: 47 73 90 40 00
Telefax 47 73 92 16 20

REPORT

Report no.: 2011.021 | ISSN 0800-3416 | Grading: Confidential to 31.12.2012

Title:
Potential of rare earth element and Zr-, Be-, U-, Th-, (W-) mineralisations in central and northern Nordland – Part 2

Authors:
Axel Müller

Client:
Nordland Mineral

County:
Nordland

Commune:

Map-sheet name (M=1:250.000)
Bodø, Sulitjelma, Svolvær, Narvik

Map-sheet no. and -name (M=1:50.000)
-

Deposit name and grid-reference:
-

Number of pages: 56 Price (NOK): 373,00 NOK
Map enclosures:

Fieldwork carried out:	Date of report:	Project no.:	Person responsible:
21.-29.09.2010	01.02.2011	305600	Rognvald Boyd

Summary:
In this report results of the investigation of potential rare earth element (REE) and Zr-, Be-, U-, Th-, (W-) mineralisations in central and northern Nordland are presented. The investigated and sampled mineralisations were proposed in NGU report 2009.037 on the basis of existing reports and geochemical data sets. The investigation targets were evolved Proterozoic TIB-type granites (TIB = Trans-Scandinavian Igneous Belt) of the Tysfjord, Sommerset and Rishaugfjell basement windows, in particular, the Hatten-Tilthornet massif, Hundholmen, Kjerrfjellet, Hellemobotn, Reinoksskardet, upper Gjerdalen areas, the Sommerset basement window, Rismålsvatn, and Memaurvatn. The general aim was to identify Zr-REE mineralisations with ≥2 wt.% REO (including Y_2O_3; REO – rare earth oxides) which are possibly enriched in Be, U and Th as well.
The field work was carried out from 21st to 29th September in 2010 as part of the project Nordland Mineral, represented by T. Vrålstad. In the field a RS-121 gamma-ray scintillometer was used in order to identify gamma radiation anomalies. 33 granite gneiss samples were collected and analysed at ACME laboratories in Vancouver, Canada, including 14 major elements and 45 trace elements. REE-bearing minerals were identified and semi-quantitatively analysed in 10 thin sections with a LEO 1450VP scanning electron microscope (SEM) at NGU.
REO+Y_2O_3 concentrations of the investigated TIB granite gneisses vary from 0.004 to 0.203 wt.%. The highest average REO+Y_2O_3 concentrations are in the granite gneisses at Hellemobotn and Reinoksskardet - 0.15 and 0. 12 wt.%, respectively. The concentrations are far below the level of economic concentrations and, thus, the detected anomalies are not of economic interest. However, compared with the average REO+Y_2O_3 concentration of Ca-poor granites, which is 0.031 wt.% according to Turekian and Wedepohl (1961), the Tysfjord granite gneisses are up to 5 times enriched in REO+Y_2O_3. The strong REE enrichment of the Tysfjord granite gneisses is remarkable from a scientific point of view and it is not clear which processes caused the REE-enrichment in the granites. The major carriers of the REE are allanite (LREE), zircon (HREE), and apatite (LREE). Titanite is presumably also an important LREE carrier in the Sommerset and Hellemobotn granite gneiss. Average grain sizes are 60 µm for allanite, 40 µm for zircon, 60 µm for apatite, and 200 µm for titanite. In addition, two important findings were made. Firstly, granite gneiss with high-gamma-ray signals are not necessarily enriched in REE and, secondly, fluids which are responsible for the U-mineralisation in the Sommerset granite gneiss leached REE from the rock.

Keywords: Technical report	REE	rare metals
Trans-Scandinavian Igneous Belt	Nordland	Tysfjord
Rishaugfjell		

Contents

Figures

Tables

Appendix

1. Introduction

Results of the investigation of potential rare earth element (REE) and Zr-, Be-, U-, Th-, (W-) mineralisations in central and northern Nordland between Mo i Rana in the south and Ofotfjorden in the north (Fig. 1) are presented in this report. The investigated and sampled mineralisations were proposed in the NGU report 2009.037 "Potential for rare earth element and Zr-, Be-, U-, Th-, (W-) mineralisations in central and northern Nordland" on the basis of existing reports and geochemical data sets (Müller 2010). The field work was carried out from 21st to 29th September in 2010 as part of the project Nordland Mineral, represented by T. Vrålstad. The general aim is to identify Zr-REE mineralisations with ≥2 wt.% REO (including Y_2O_3; REO – rare earth oxides) which are possibly enriched in Be, U and Th as well.

The major outcome of NGU report 2009.037 was that some of the more evolved Proterozoic TIB-type granites (TIB = Trans-Scandinavian Igneous Belt) of the Tysfjord, Sommerset and Rishaugfjell basement windows have the potential for sub-economic to economic Zr-REE-mineralisations. Based on these results the suggested target areas for sampling were the Hatten-Tilthornet massif (Ulsvåg), the Hundholmen peninsula, the Kjerrfjellet (Drag), the Hellemobotn, the Reinoksfjellet, the upper Gjerdalen, the Sommerset areas (Kalvik window according to Hansen [1983]), the area NW of the Faulevatn, and the northern part of the Rishaugfjell basement window (Memaurvatn; Fig. 2). Because, of the limited time in the field and difficult access, equivalents of the Reinoksfjellet and Faulevatnet Tysfjord granite gneisses were sampled at Reinoksskardet and Rismålsvatn, respectively. In addition, the Lagmannsvik pegmatite, located at the western contact of the Tysfjord basement window and the Kalvik granite was examined. The Kalvik granite has been considered as Proterozoic basement granite (e.g. Solli and Nordgulen 2006) or as metaarkose (Gustavson et al. 2004). However, field observations during this project indicate, that the Kalvik granite is a fine-grained, presumably Caledonian biotite granite (see chapter 4.1). Summarizing, the following localities were investigated and sampled during the field work in September 2010 (Fig. 2):

1) Northern Rishaugfjell window
    - Memaurvatn
2) Southern Tysfjord window:
    - Kalvik granite
    - Sommerset window
    - Rismålsvatn
3) Central Tysfjord window:
    - Gjerdalsvatn
    - Reinoksskardet
    - Hellemobotn
    - Lagmannsvik pegmatite
4) Northern Tysfjord window:
    - Hundholmen peninsula
    - Kjerrfjellet
    - Hatten-Tilthornet massif

The localities are described in the following in the order as show above. The regional geology of the investigated area is explained in the NGU report 2009.037.

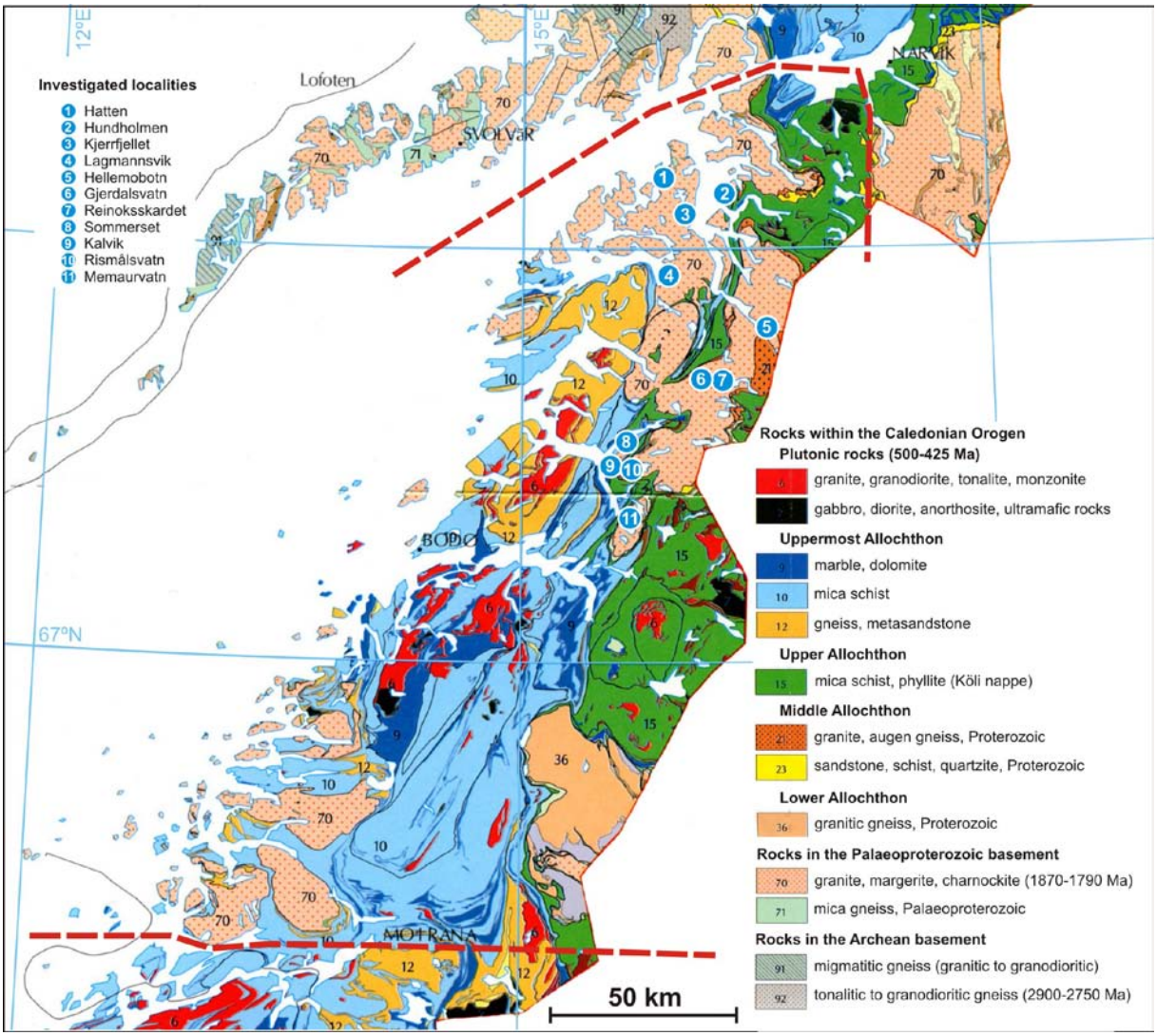

Figure 1. *Geological map of central and northern Nordland according to Solli and Nordgulen (2006) with the investigated localities. The dashed lines frame the area considered in NGU report 2010.037.*

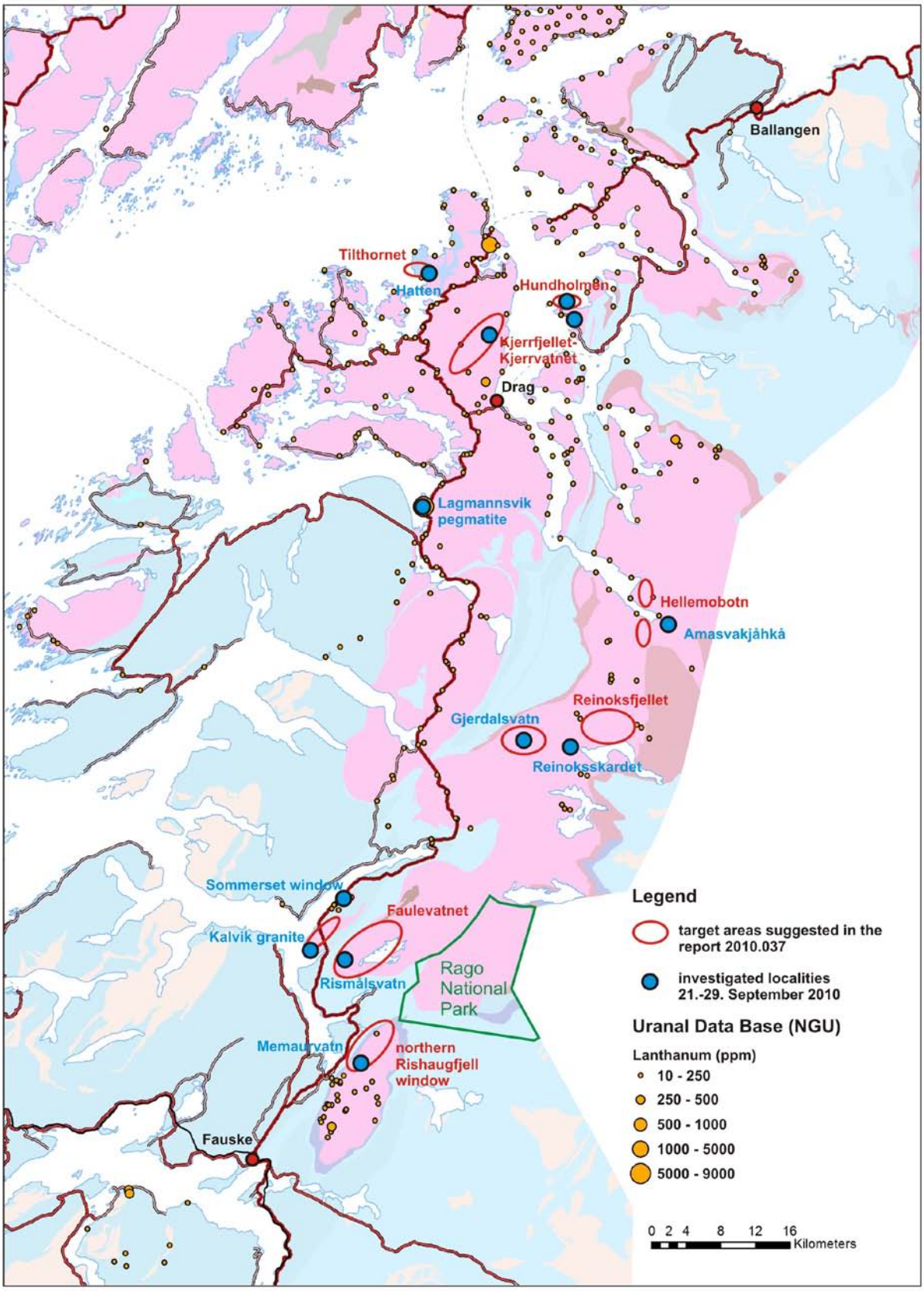

Figure 2. *Simplified geological map of northern Nordland with supposed and investigated target areas and with La concentrations of rock samples (yellow dots) registered in the NGU Uranal data base. The pink areas are the basement windows comprising predominantly deformed and undeformed TIB-granites.*

2. Methods

2.1 Scintillometer measurements

In the field a RS-121 gamma-ray scintillometer from Terraplus Inc. was used in order to identify gamma radiation anomalies. Principally, the natural gamma radiation is caused by the decay of Th, U and K isotopes. REE minerals commonly contain Th and in some cases U and, therefore, the gamma-ray intensity is an indicator for REE enrichments. The portable scintillometer is equipped with large 2.0 x 2.0 Nal crystal (103 cm^3) which allows sensitive measurements in the field. Besides the radiation intensity measured in counts per second (cps) the approximate concentrations of Th, U and K are determined in situ by attaching the scintillometer detector to the clean rock face. In the diagram in Figure 3 the scintillometer measurements carried out during the field work in September 2010 are plotted.

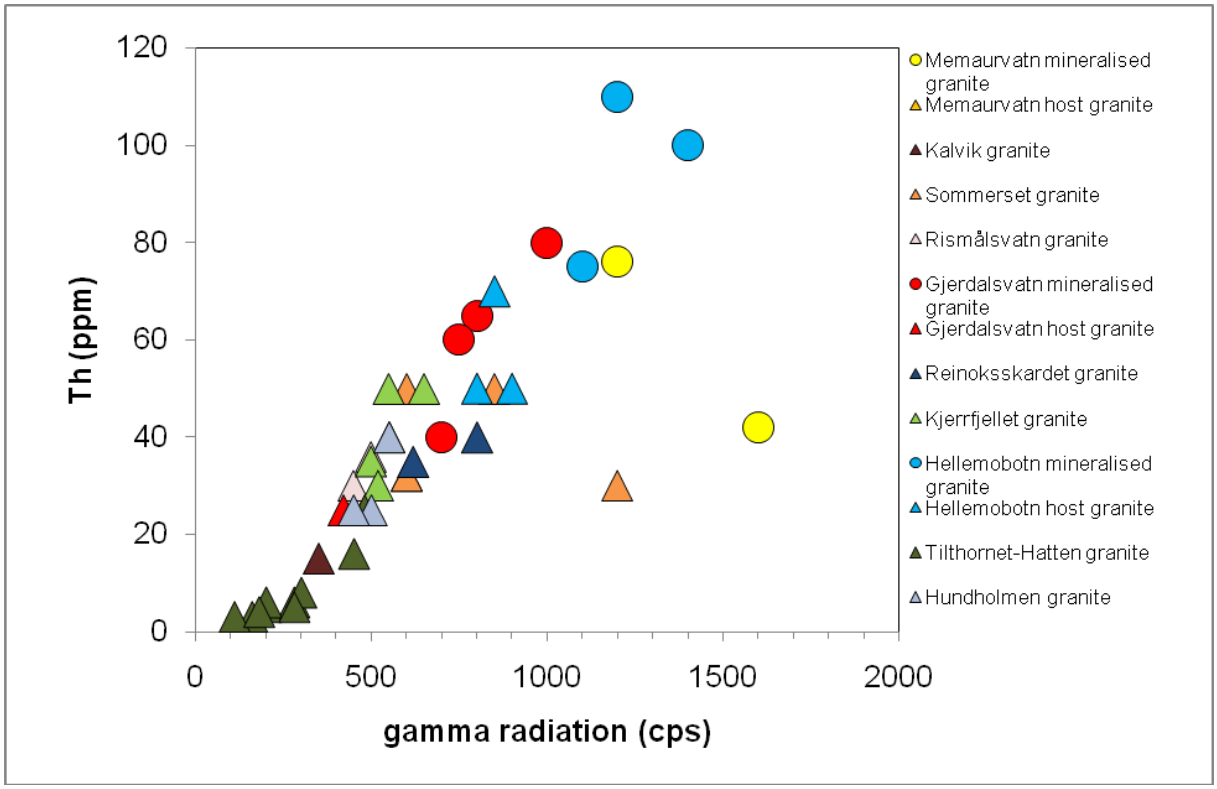

Figure 3. *Diagram of the gamma-ray intensity versus Th concentration of non-mineralised (triangles) and mineralised (circles) TIB-type granites and the Caledonian (?) Kalvik granite. The data were collected with the scintillometer in the field. The Th concentrations are calculated from the counts of Th isotopes and, thus, the concentrations have a large error (about 25%).*

2.2 Whole rock analyses

33 granite samples were analysed at ACME laboratories in Vancouver, Canada (Appendix 1). The analyses include 14 major elements and 45 trace elements including all REE (analysis code 4A4B) (Appendix 2). The sample characterization comprised four separate analytical tests. Total abundances of the major oxides and several minor elements were reported on a 0.2 g sample analysed by ICP-emission spectrometry following a Lithium etaborate/tetraborate fusion and dilute nitric digestion. Loss on ignition (LOI) was determined by weight difference after ignition at 1000°C. Rare earth and refractory elements were determined by ICP mass spectrometry following a lithium metaborate/tetraborate fusion and nitric acid digestion of a

0.2g sample. In addition, a separate 0.5 g split was digested in aqua regia and analysed by ICP mass spectrometry to report the precious and base metals.

2.3 Scanning electron microscopy

REE-bearing minerals were identified and semi-quantitatively analysed on polished and carbon-coated thin sections with a LEO 1450VP scanning electron microscope (SEM) at NGU. The standard petrographic thin sections were produced from 10 representative samples in the preparation laboratories of Dettmar in Bochum, Germany. The SEM is equipped with an Oxford Instruments energy dispersive X-ray (EDX) detector. The applied acceleration voltage and current were 20 kV and ~1 nA, respectively. INCA software was used for the EDX spectra acquisition and semi-quantitative calculation of mineral compositions. Backscattered electron images (BSE) were taken of REE-bearing accessory minerals.

3. Northern Rishaugfjell window

3.1 Memaurvatn

The reason for sampling the granite gneiss of the northern Rishaugfjell window was one Uranal database analysis of a TIB-granite sample from Memaurvatn (UTM 33W 529233E/7472096N) which contained 11700 ppm Zr and 884 ppm Y+La+Ce. During the field campaign two areas of coarse-grained biotite granite gneiss (ca. 130 x 30 m and 150 x 5 m) with high gamma radiation (>1000 cps) were identified south of the lake Memaurvatn (Figs. 4 to 6). The estimated resource is about 300 000 tons assuming a vertical extension of the mineralisation of 25 m. The mineralised granite gneiss contains aggregates of fine-grained violet fluorite with crystal sizes of up to 1 mm (Fig. 7). The gamma radiation of the non-mineralised, fluorite-free host granite gneiss is about 480 cps.

Three samples were collected: two mineralized coarse-grained biotite granite gneisses (samples 22091002 and 22091003) and one non-mineralised coarse-grained biotite granite gneiss (sample 22091001). All three samples have REO concentrations of 0.064 to 0.070 wt.% REO (Fig. 8). Sample 22091001 is characterized by high Zr - 1658 ppm and high U - 134 ppm (Appendix 2). The REE distribution pattern indicates that LREE and HREE are enriched in samples 22091001 and 22091002 compared to average granite composition according to Turekian and Wedepohl (1961) (Fig. 9). In addition, the Memaurvatn granite gneiss is characterized by a strong Eu anomaly indicating a strong fractional crystallization. The fluorite-bearing sample 22091003 is slightly depleted in HREE. It is assumed, that the fluorite-forming fluids caused the HREE depletion in sample 22091003. Thus, high gamma-ray signals measured with the scintillometer in the field do not necessarily detect all rocks with elevated REE-Zr concentrations.

SEM investigations revealed that allanite and zircon are the most common accessory REE-bearing minerals (Fig. 10, Table 1). Fluorite is particularly common in sample 22091003 but it contains <1 % REE. Apatite, monazite or xenotime, which are common accessories in granitic rocks, could not be identified. Allanite crystals are 40 to 120 µm in size and carry most of the LREE. Zircon forms two generations: an older, porous, partially dissolved generation, with grain sizes of 20 to 80 µm and younger, euhedral, homogeneous generations with grain sizes of 5 to 10 µm. Zircon is the major carrier of the HREE. In addition there are some titanite crystals, 10 to 50 µm. In sample 22091003 zircons of generation 1 are most intensely dissolved which explains the depletion of HREE. Titanite can be an important carrier of LREE (e.g. Seifert 2005) but EDX analysis revealed that the REE content of the titanites is <1 wt.%.

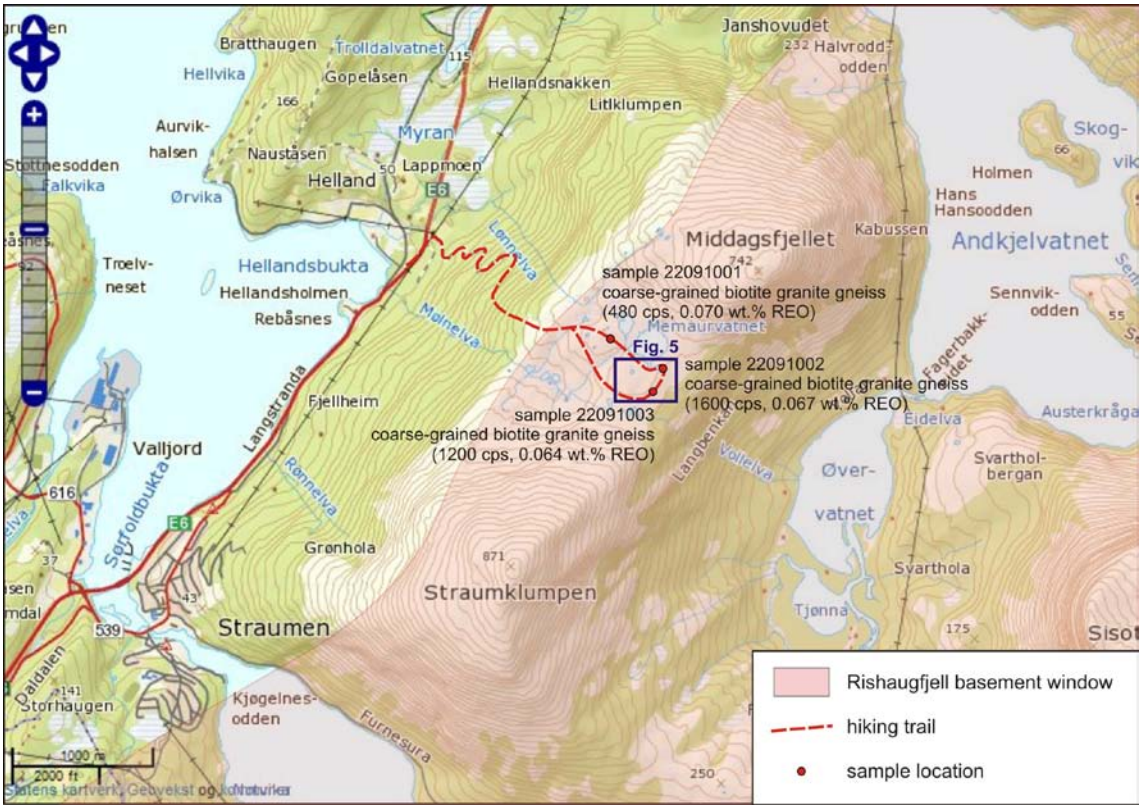

Figure 4. *Hiking trail and sampling locations at Memaurvatn in the northern Rishaugfjell basement window.*

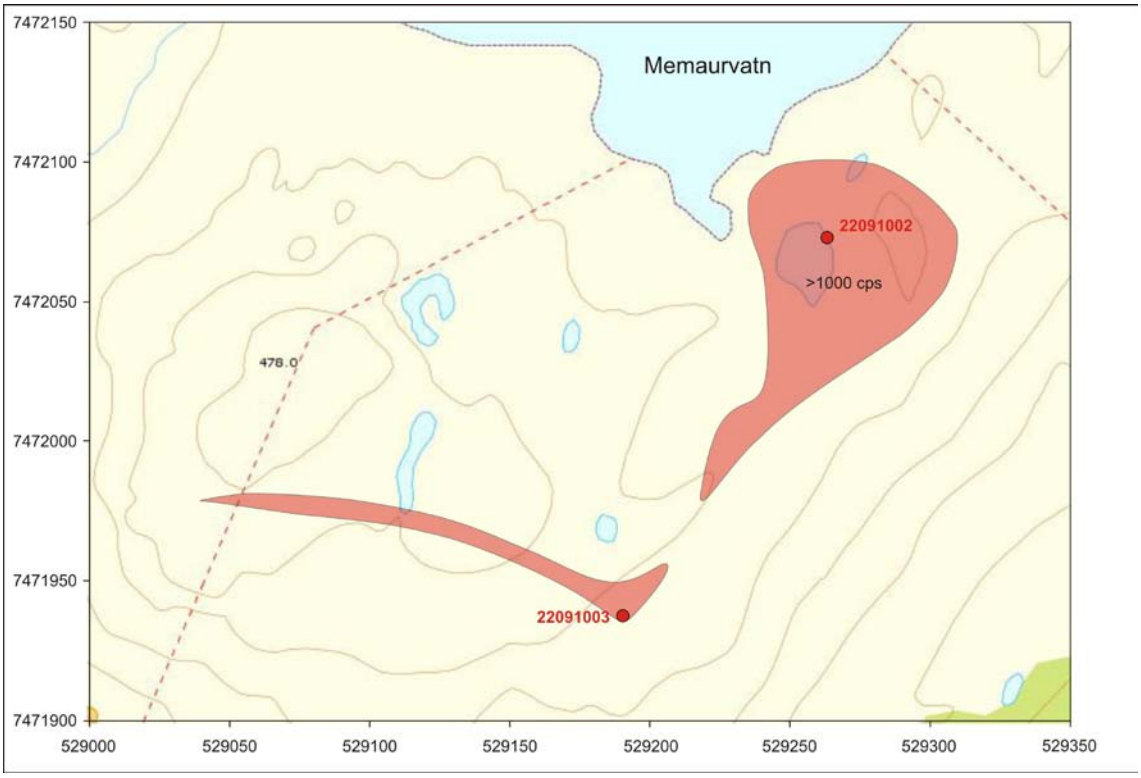

Figure 5. *Extension of the biotite granite gneiss with high gamma-ray intensity of >1000 cps (red areas) at Memaurvatn.*

Figure 6. *a – The Rishaugfjell basement window at Memaurvatn with a view towards the north to Middagsfjellet. The mineralised granite gneiss is exposed in the foreground. b – Scintillometer measurement of the mineralised granite at Memaurvant (1104 cps).*

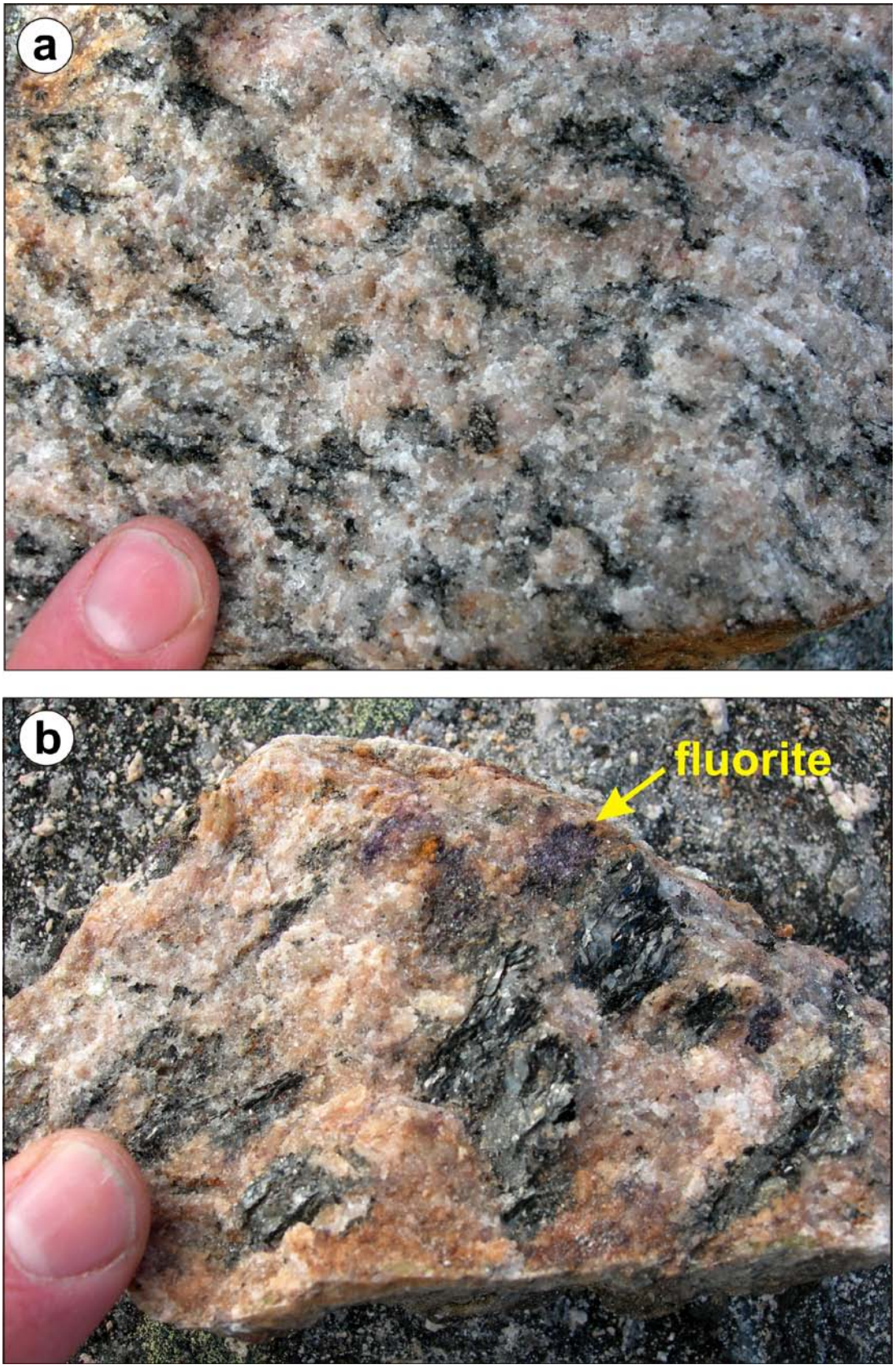

Figure 7. *a – Typical biotite granite gneiss at Memaurvatn (sample 22091001). b - Coarse-grained biotite granite gneiss with violet fluorite (sample 22091003). The sample has a high gamma-ray emission of 1200 cps but slightly lower REO concentrations than sample 22091001 which had a gamma-ray emission of 480 cps.*

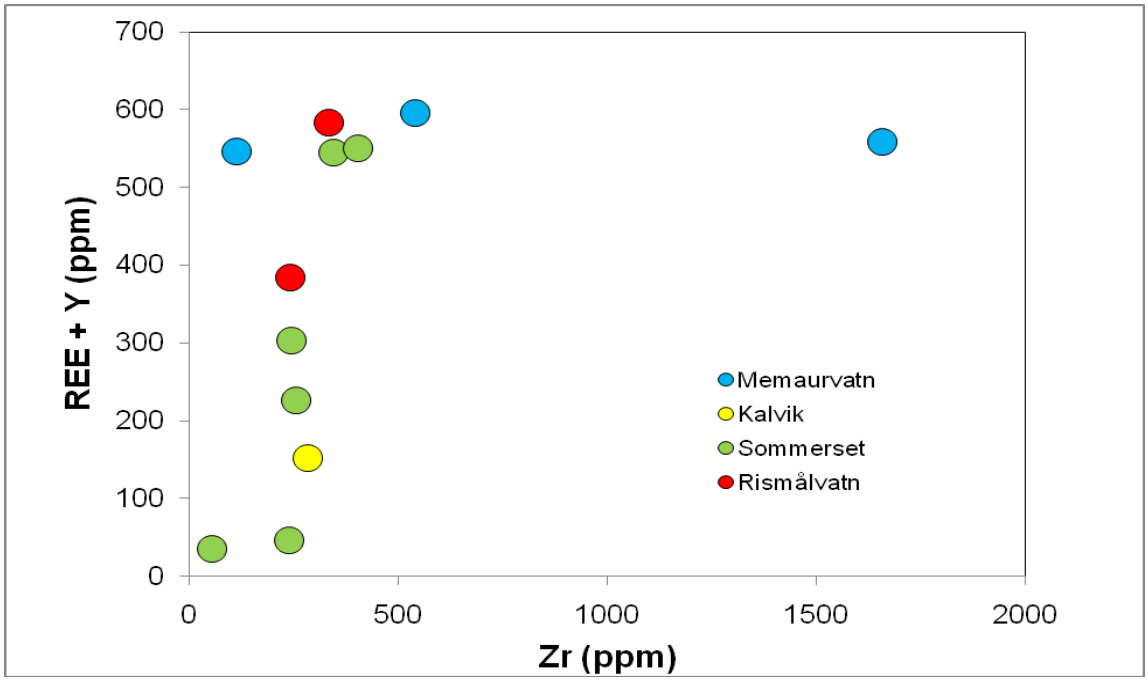

Figure 8. *Concentrations of Zr versus REE + Y of biotite granite gneisses from the Rishaugfjell window and the southern Tysfjord window. The mineralised granite gneisses have >500 ppm REE+Y.*

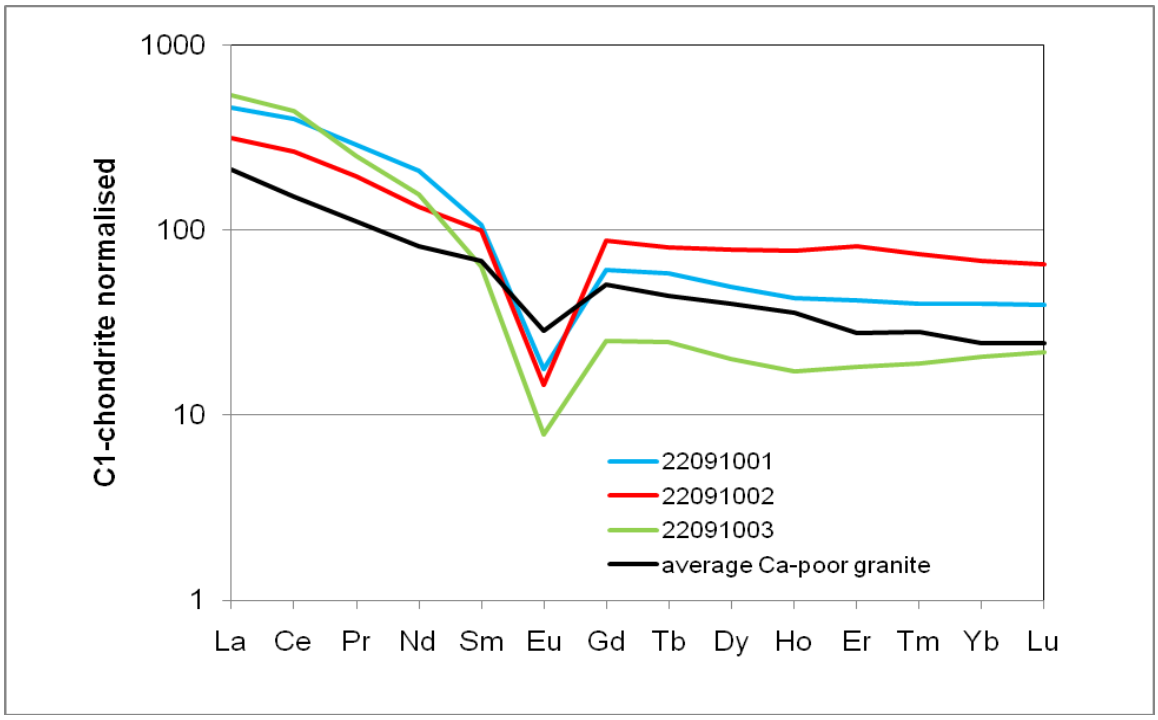

Figure 9. *Chondrite-normalised REE pattern of the Memaurvatn samples compared with the pattern of average Ca-poor granites modified after Turekian and Wedepohl (1961). The fluorite-bearing sample is slightly depleted in HREE.*

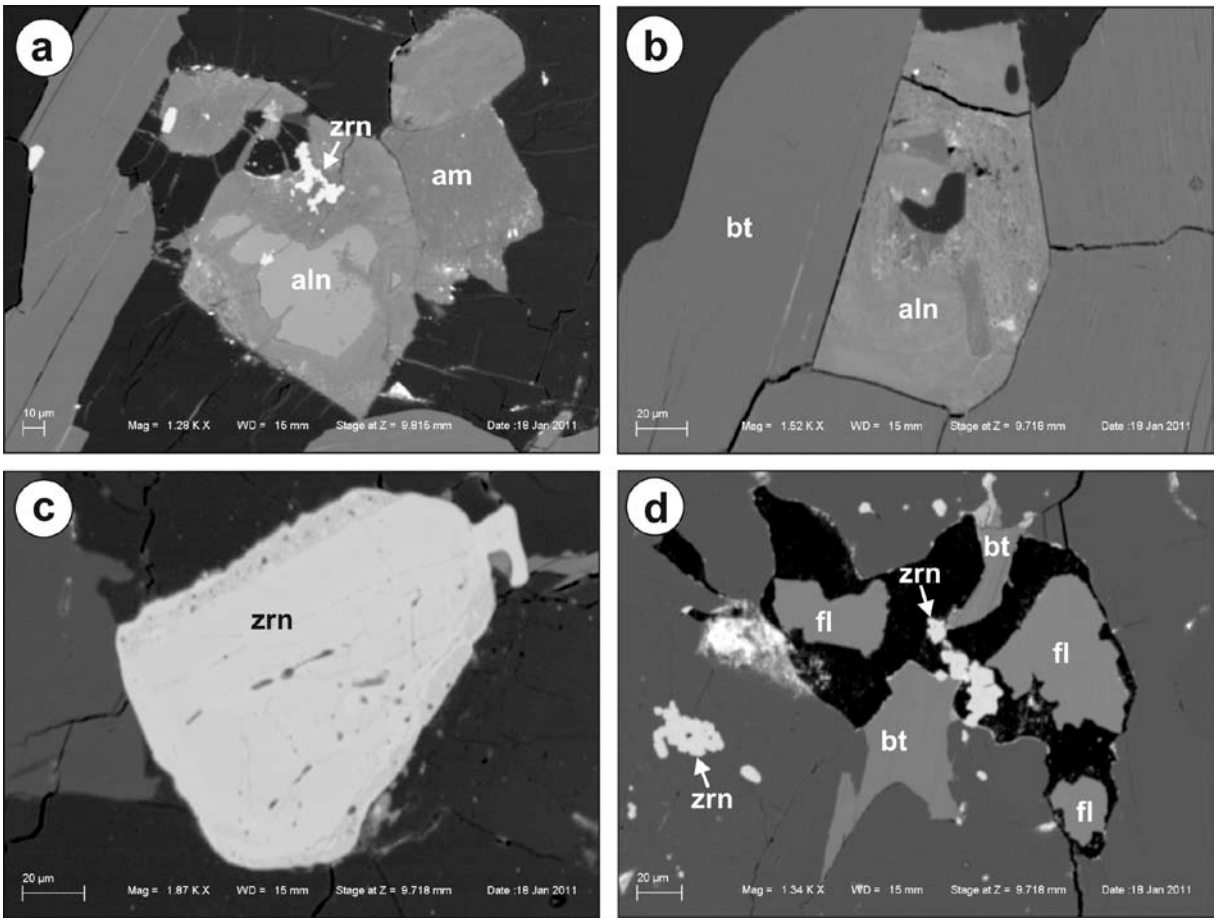

Figure 10. *BSE images of accessory REE-bearing minerals in the Memaurvatn granite gneiss. a – Th-rich allanite (aln) with alteration zoning with inclusions of second-generation zircons (zrn). am- amphibole. b – Th-poor allanite surrounded by biotite (bt). c – Corroded first-generation zircon. d – Cavity with fluorite (fl) and second-generation zircon (zrn) and dissolved biotite (bt).*

Table 1. REE-Zr-Th-U-bearing accessory minerals in TIB-type granite gneisses identified by SEM and EDX. These minerals have a sum contribution to the whole rock REE- Zr-Th-U-budget of 95% (Bea 1996). The description "homogeneous" mineral refers to non-visible growth and alteration zoning in the BSE images.

Mineral	**Memaurvatn**	**Sommerset**	**Gjerdalsvatn**	**Reinoksskardet**	**Hellemobotn**	**Kjerrfjellet**
allanite	very common, 40-120 µm, subhedral, alteration zoning	very common, 40-200 µm, subhedral, primary and alteration zoning	very common, 20-80 µm, subhedral, primary and alteration zoning	very common, 20-250 µm, subhedral, primary and alteration zoning	very common, 20-40 µm, subhedral, replaced by titanite, Th-rich (7 wt.%) and Ca-poor	-
zircon	common, two generations: 1) 20-80 µm, porous, dissolved 2) 5-10 µm, euhedral, homogeneous	very common, 20-200 µm, subhedral, porous, zoned	very common, 20-60 µm, subhedral, porous, homogeneous	very common, 20-120 µm, euhedral, porous, zoned	Very common, 20-160 µm, anhedral, porous, strongly dissolved/corroded	very common, 20-60 µm, euhedral, homogeneous
apatite	-	common, 20-100 µm, subhedral, homogeneous	common, 40-100 µm, subhedral, homogeneous	common, 20-60 µm, subhedral, homogeneous	very common, 20-60 µm, subhedral, homogeneous	very common, 20-300 µm, subhedral, homogeneous
titanite	rare, 10-50 µm, euhedral, homogeneous	very common, 10-500 µm, euhedral, slightly zoned	-	-	very common, 40-2000 µm, subhedral, zoned	-
fluorite	common, 20-100 µm, anhedral, homogeneous, dissolved	rare, 30-60 µm, anhedral, homogeneous, dissolved	-	-	rare, 20-200 µm, anhedral, homogeneous, partially dissolved	-
magnetite	-	-	-	-	common, 40-1000 µm, euhedral, homogeneous	-
synchysite	-	common, 5-50 µm, subhedral, zoned, formed by secondary processes	-	-	-	-
other rare minerals	-	-	-	rare, thorite, uraninite, 5-20 µm	rare, polycrase-(Y), thorianite, 5-10 µm	common, almandine-like minerals with 1 wt.% P and Cl, 60-100 µm

4. Southern Tysfjord window

4.1 Kalvik granite

The Kalvik granite is a fine-grained, slightly foliated biotite granite, which extends 5 km in SW-NE direction from the village Aspenes to the Klimpen mountain and 1.5 km in NW-SE direction (Fig. 11). The term Kalvik granite is being introduced by the author due to some confusion in the literature. The granite has been considered as a Proterozoic TIB-granite forming a small (5 x 1.5 km) basement window (e.g. Solli and Nordgulen 2006) or as metaarkose belonging to the Caledonian Gasak Nappe Complex (Gustavson et al. 2004). The field observations indicate that the exposed rocks are slightly foliated, fine-grained biotite granites (Fig. 12). Their macroscopic appearance is different from the TIB-granites as regards degree of deformation and mineralogy. The contact relationships between the Kalvik granite and the Caledonian metasediments indicate that the granite is presumably of Caledonian age (syn- to late-orogenic). The Kalvik granite has a typical granitic composition with 0.018 wt.% REO(+Y_2O_3), 284 ppm Zr, 10 ppm Th and 4 ppm U (Fig. 8). The REEs are slightly depleted compared to the average granite composition (Fig. 13). The Kalvik REE pattern is very different from the TIB-type granite gneisses, supporting the statement that the Kalvik granite has a different origin and age. SEM investigations were not carried out because the granite has obviously no potential for REE-mineralisations.

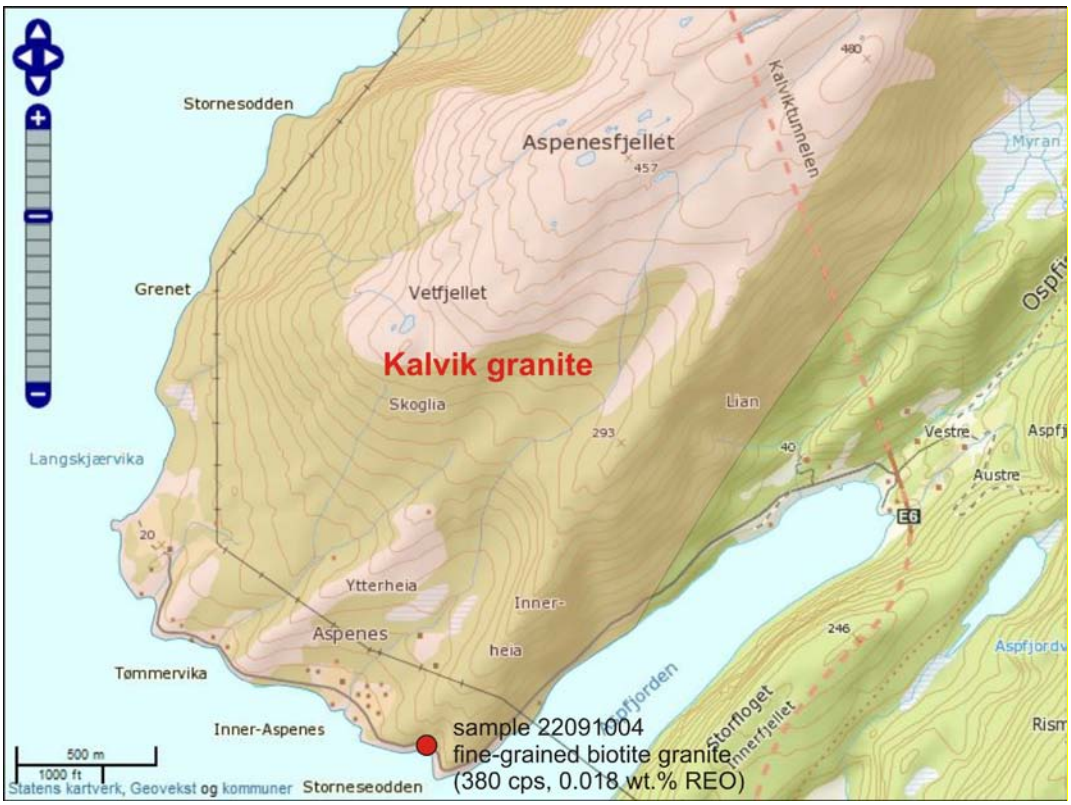

Figure 11. *Extension of the Kalvik granite (pinkish area), which is interpreted as syn- to late-orogenic Caledonian granite. The red dot indicates the sample location with gamma-ray intensity in cps and REO content.*

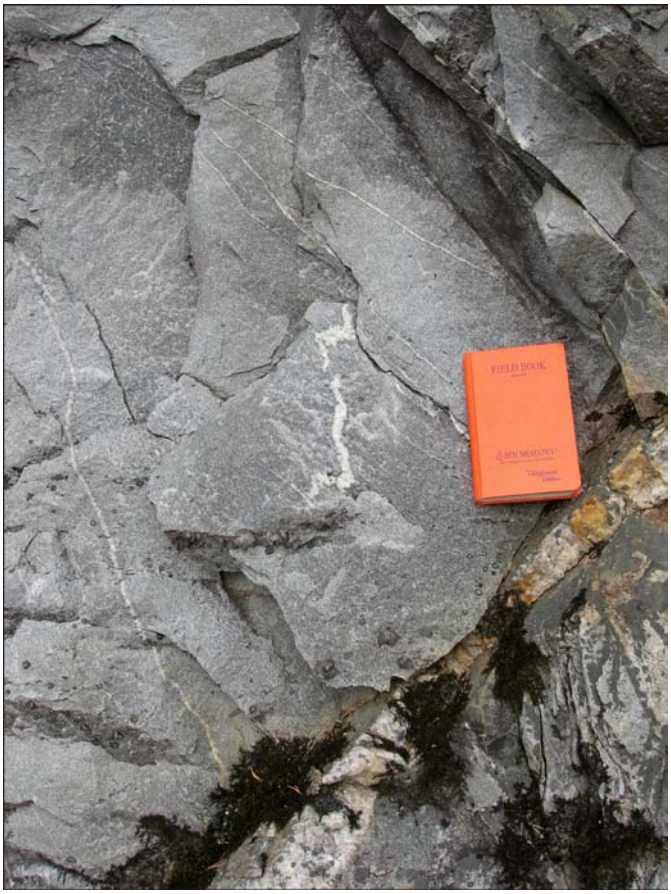

Figure 12. *Exposure of fine-grained Kalvik granite with different generations of quartz veins. The large quartz vein contains sulphides.*

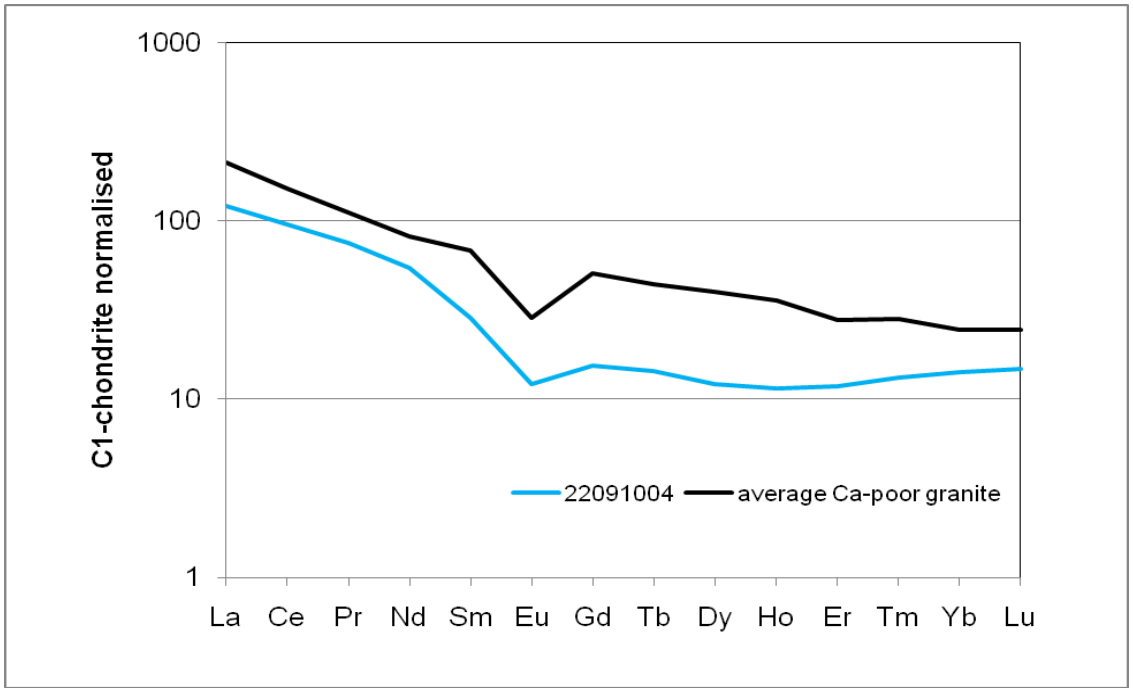

Figure 13. *Chondrite-normalised REE pattern of the Kalvik granite compared with the pattern of average Ca-poor granites modified after Turekian and Wedepohl (1961).*

4.2 Sommerset window

The Sommerset window is a small basement window immediately SW of the Tysfjord window, exposing granite gneisses of the TIB-type in an area of approx. 3 km^2. Hansen (1983) named the basement window Kalvik window. However, in this report the term Sommerset window is applied according to Stendal (1990) because the window is close to the village, Sommerset.

There were two reasons for sampling the TIB-granites of the Sommerset window: Firstly, the description of minor Mo-U-(W) mineralisations at the contact between the granite gneiss and Caledonian meta-sediments by Hansen (1983) and , secondly, the statement by Stendal (1990) that the mineralised Sommerset granite gneiss contains up to 1.3 % Zr, 0.9% Ce, 0.45 % La, 0.35 % Nd, 0.2 % Y, 0.16 % Th, and 0.1 % Nb. Hansen (1983) reported an average granite gneiss composition of 10 ppm U, 35 ppm Th, 5 ppm Mo, 288 ppm Zr, 21 ppm Nb, and 51 ppm Y (average of 7 analyses).

Figure 14 shows the sample locations and the uranium-molybdenite (U-Mo) and magnetite (Mt) mineralisations according to Hansen (1983). Two samples were collected at the SE contact of the window (samples 22091005 and 22091006) where the rock shows gamma-ray intensities of 600 cps (away from the basement window contact) and 850 cps (close to the basement window contact). The second batch of samples (22091007-10) was collected at the north contact of the basement window, where small U-Mo mineralisations were reported by Hansen (1983) (Fig. 15). Gamma-ray intensity increases up to 1200 cps on up to 1-m-sized areas in granite gneiss close to the contact and on pegmatite lenses in megaschists immediately above the contact.

The REO content varies from 0.004 to 0.064 wt.%, Zr - 54 to 402 ppm, Mo - 0 to 79 ppm, U - 7 to 121 ppm and Th - 4 to 42 ppm (Fig. 8, Appendix 2). The pegmatite sample 22091010 shows the highest Mo - 79 ppm, As - 14 ppm and U - 121 ppm but the lowest REO - 0.004 wt.%. The samples 22091008 (granite gneiss with high gamma-radiation of 1000 cps) and 22091010 (pegmatite lens) have an unusual, depleted REE pattern caused by secondary REE mobilization by fluids which may be responsible for the U and Mo enrichment (Fig. 16). The high REE-Zr-Th values in the mineralised Sommerset granite reported by Stendal (1990) could not be confirmed. Also these results reveal that high gamma-radiation signals are not necessarily indicative for elevated REE-Zr concentrations.

The dominant accessory REE-bearing minerals in the Sommerset granite gneiss are allanite (40-200 µm), zircon (20-200 µm), apatite (20-100 µm) and titanite (10-500 µm) (Fig. 17). Synchysite occurs as small (5-50 µm) grains as alteration product of dissolved allanite (Figs. 17b, c). Fluorite occurs occasionally as a secondary mineral.

It is important to note that the fluids responsible for the U-Mo mineralization caused the depletion of REE in the rock and, thus, the rocks with the highest gamma-radiation signal are depleted in REE. In conclusion, the rocks of the Sommerset window have no potential for economic REE-Zr mineralization.

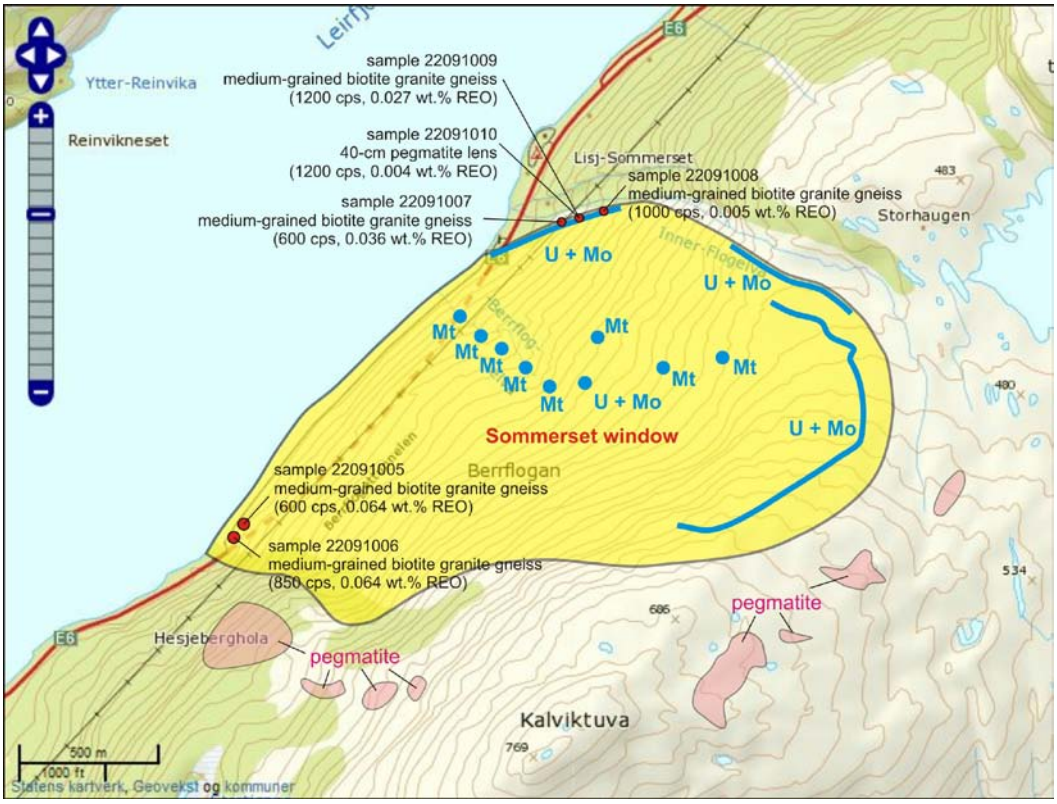

Figure 14. *Extension of the Sommerset window (yellow) with minor uranium-molybdenite (U-Mo) and magnetite mineralisations (Mt; blue) and pegmatites (pink) according to Hansen (1983) and sampling locations (red dots) with gamma-ray intensity in cps and REO content.*

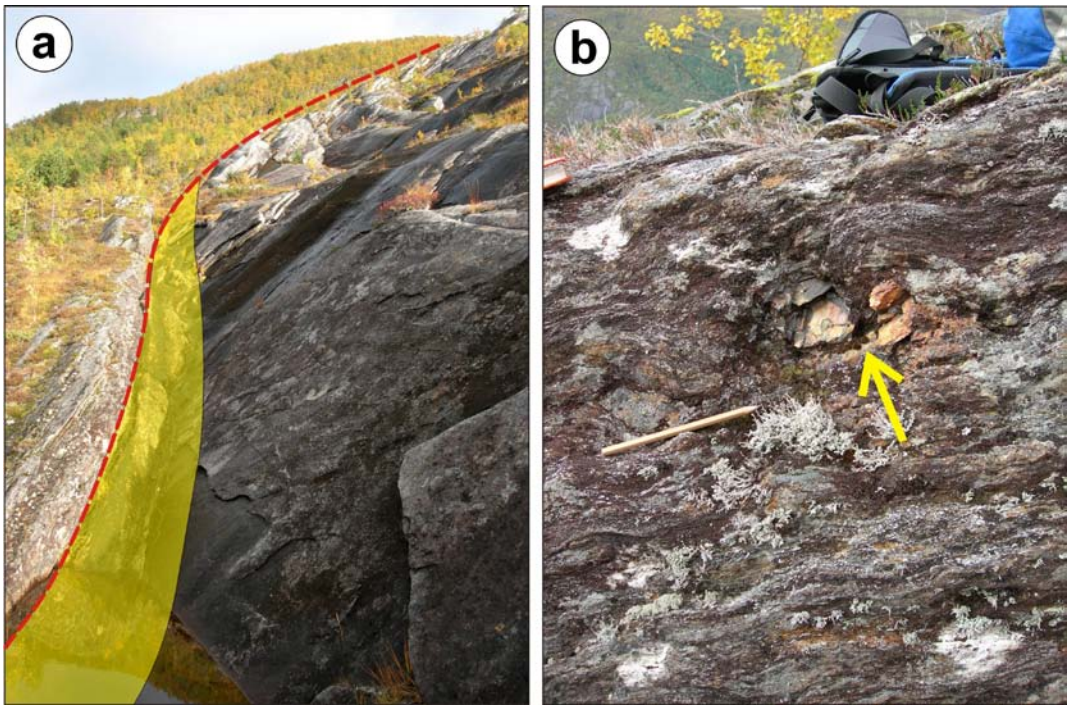

Figure 15. *a – Northern contact (red dashed line) of the Sommerset basement with the TIB-type granite gneiss on the right and mica schist on the left. The yellowish shaded zone indicates slightly mineralized granite gneisses from which the samples 22091007-09 originate. View towards NW. b – 40-cm pegmatite lens in mica schist immediately above the contact to the basement window.*

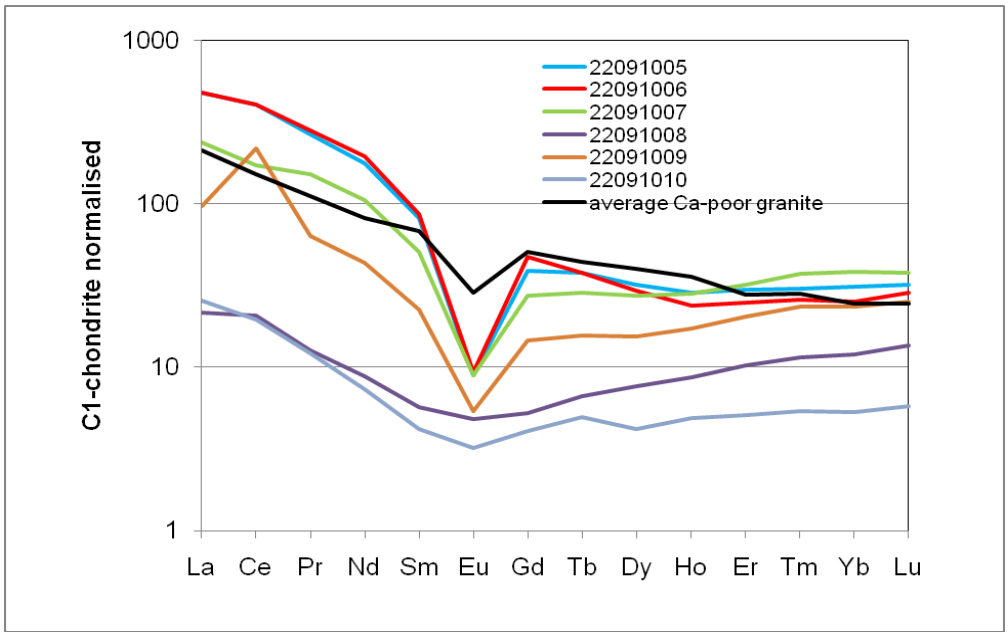

Figure 16. *Chondrite-normalised REE pattern of the Sommerset granite gneiss compared with the pattern of average Ca-poor granites modified after Turekian and Wedepohl (1961).*

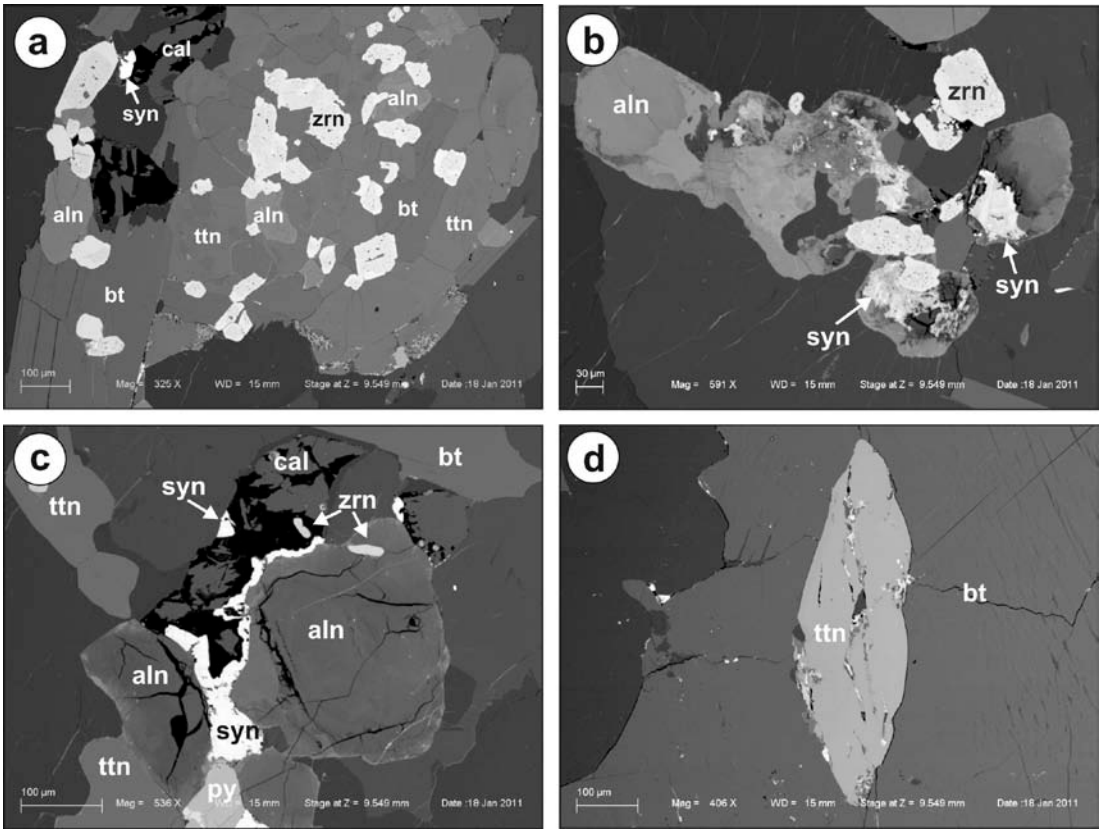

Figure 17. *BSE images of accessory REE-bearing minerals in the Sommerset granite gneiss. a – Cluster of biotite (bt), titanite (ttn), zircon (zrn) and allanite (aln). Secondary processes resulted in the formation of synchysite (syn) and calcite (cal, upper left). b - cluster of allanite (aln) and zircon (zrn) with secondary formed synchysite (syn). c – Large, partially dissolved allanite crystal (aln). Secondary process caused the dissolution of allanite and the formation of synchysite (syn), calcite (cal) and pyrite (py). d – Large, slightly deformed titanite crystal (ttn) in biotite (bt).*

4.3 Rismålsvatn

The reason for sampling TIB-granites in the area of Rismålvatn was the statement by Stendal (1990) that the most evolved TIB-granites occur in the southernmost Tysfjord window and, thus, they are enriched in incompatible elements and presumably REE. Stendal (1990) reported strong enrichments of REE in the nearby Sommerset granite gneiss with up to 1.3 % Zr, 0.9% Ce, 0.45 % La, 0.35 % Nd, 0.2 % Y, 0.16 % Th and 0.1 % Nb and, concluded that similar enrichments may occur in the Faulevatn area. However, the reported enrichments in the Sommerset granite gneiss could not be confirmed (see chapter 4.2). In NGU report 2009.037 the area NW and W of the Faulevatnet was suggested for sampling, but because of the limited time in the field and difficult accessibility the sampling was restricted to the Rismålvatn area, W of Faulevatn (Figs. 18 and 19).

The two samples of Rismålvatn granite gneiss contain 0.046 and 0.069 wt.% REO+Y_2O_3 (Fig. 8), 242 and 332 ppm Zr, 18 and 22 ppm Th and 8 and 13 ppm U. Compared to average granite composition LREE and HREE are slightly enriched in the Rismålvatn granite gneiss (Fig. 20). The granite gneisses have a pronounced Eu anomaly indicating the strong degree of fractionation of the original granite magma. The strong REE enrichments indicated for the granite gneiss in the area by Stendal (1990) could not be confirmed. SEM-investigations were not carried out because of the common REO content. There are is no obvious potential for economic REE mineralisations in the area.

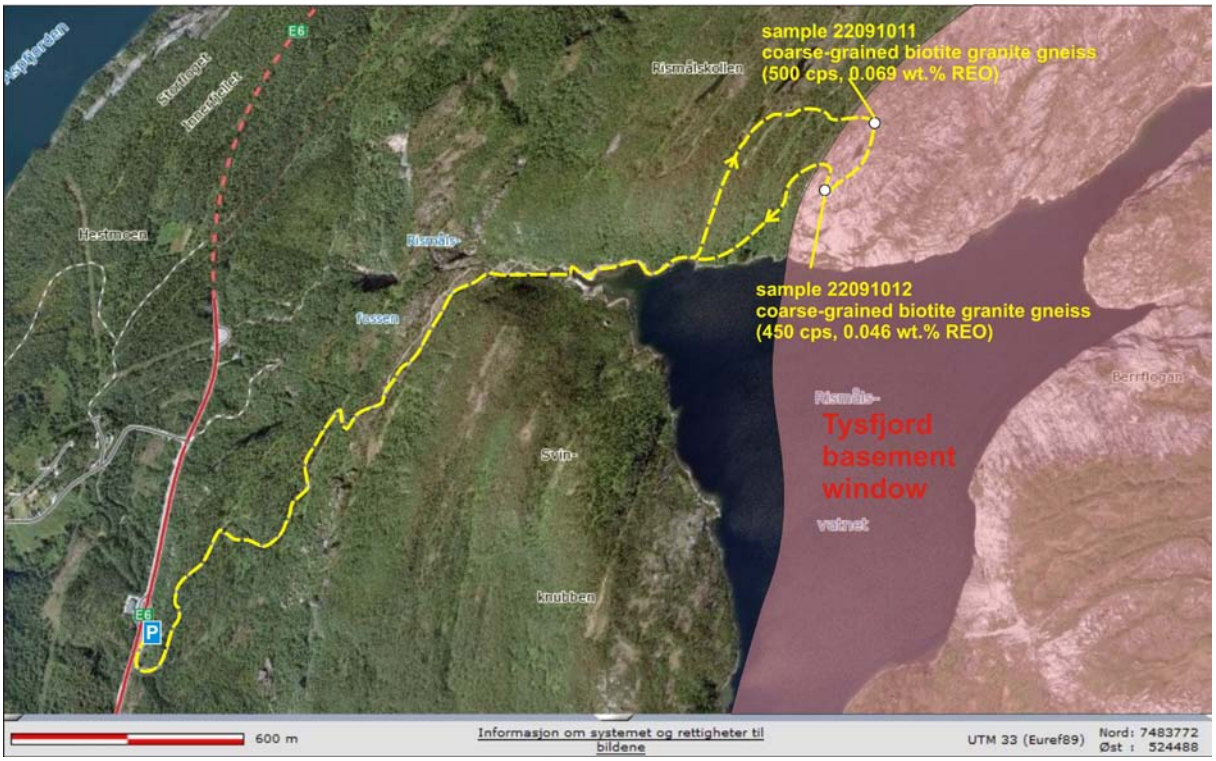

Figure 18. *Hiking trail (yellow dashed line) and sampling locations with gamma-ray intensity in cps and REO content north of Rismålsvatn. The Tysfjord basement window is pink shaded. Source of the air photograph: http://www.norgeibilder.no.*

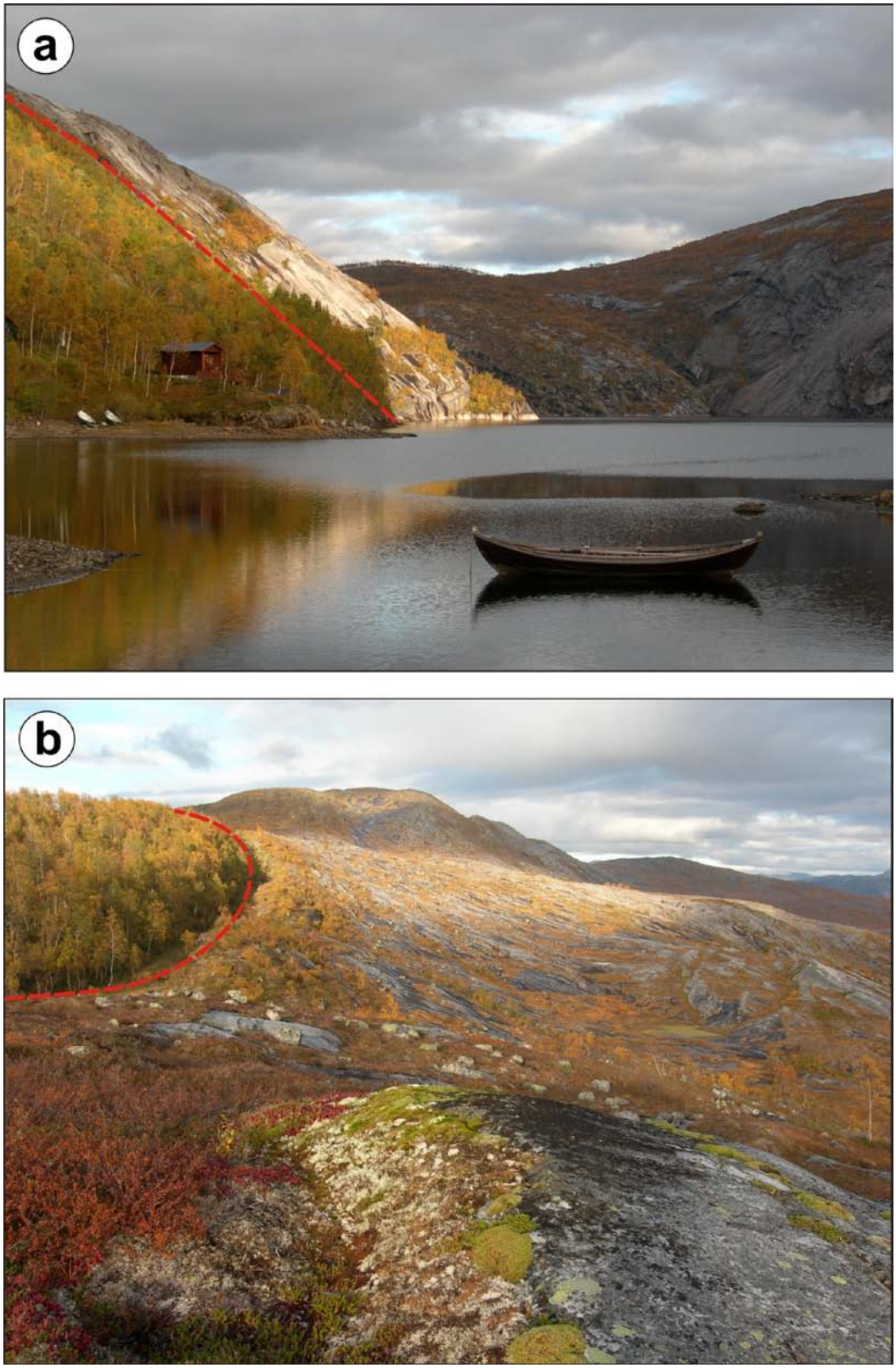

Figure 19. *a – Border of Tysfjord basement window (red dashed line) seen from the eastern shore of the Rismålsvatn. b – Sampling location of sample 22091011 in the foreground with view towards Grønfjellet. The red dashed line marks the boundary between the Tysfjord granite gneiss on the right and the Caledonian metasediments on the left.*

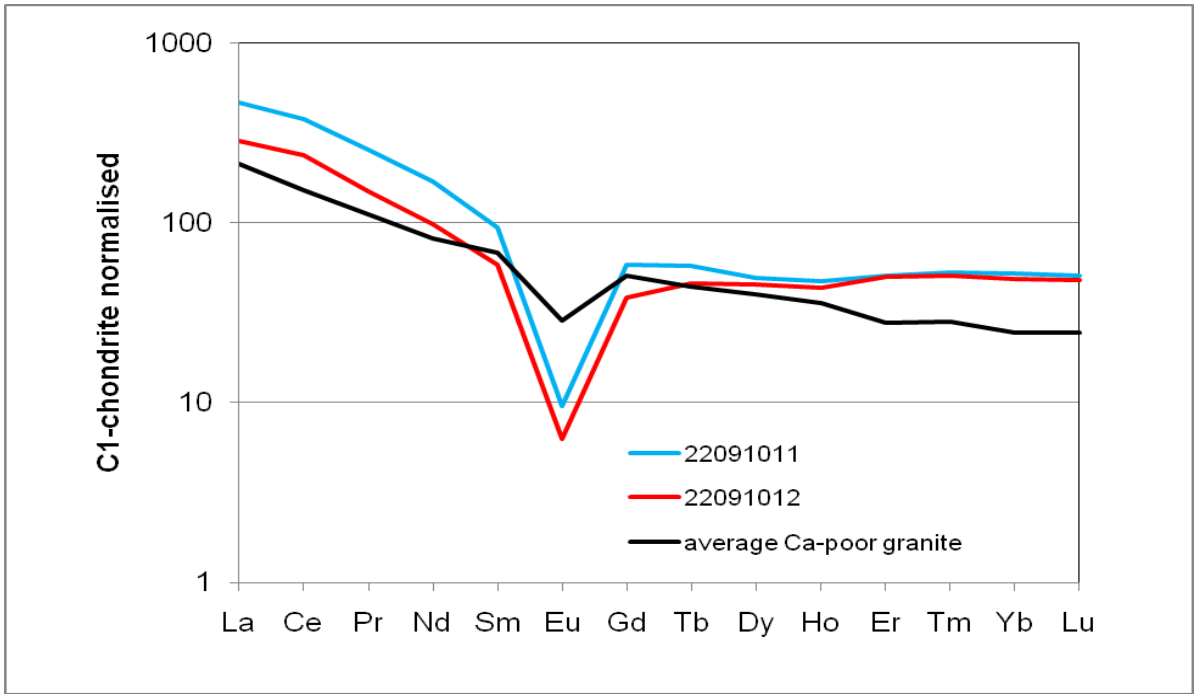

Figure 20. *Chondrite-normalised REE pattern of the Rismålvatn samples compared with the pattern of average Ca-poor granites modified after Turekian and Wedepohl (1961).*

5. Central Tysfjord window

5.1 Gjerdalsvatn

The Gjerdalsvatn locality was chosen as target area on the basis of one Uranal database analysis of granite gneiss with anomalously high La - 541 ppm and Ce - 1200 ppm (Müller 2010). The sample was collected by J. Hysingjord in the 1970s. The locality was immediately identified in the field because of high gamma-radiation of >700 cps compared to the host granite gneiss with about 400 cps. The rock with the high gamma-radiation forms a dyke-like structure which is about 600 m long and up to 20 m wide and plunges 60-70º to the S-SE (Figs. 21, 22). The estimated resource is about 150 000 tons assuming a vertical extension of the mineralisation of 25 m. It is a fine-grained, almost aplitic biotite granite gneiss which can be easily distinguished from the coarse-grained granite gneiss host (Fig. 22b). Four fine-grained granite gneiss samples (23091001, -02, -04, 28091009) and one coarse-grained granite gneiss sample (23091003) were collected. Surprisingly, the host granite gneiss (sample 23091003) has the highest REO+Y_2O_3 of 0.111 wt.% but the lowest U - 4 ppm and Th of 30 ppm, explaining the low gamma-ray intensity (Fig. 23). The fine-grained granite gneiss contain 0.010 to 0.052 wt.% REO+Y_2O_3, 164 - 230 ppm Zr, 38-56 ppm Th and 5 - 21 ppm U. In this case, the scintillometer measurements are not indicative for elevated REE concentrations. The Gjerdalsvatn granite gneisses are slightly enriched in LREE compared to average granite composition and slightly depleted in HREE (Fig. 24). Sample 28091009 is, for some reason, depleted in all REE compared to the average granite composition. The most common REE-bearing accessory minerals are allanite (20-250 µm), zircon (20-120 µm) and apatite (40-100 µm) (Fig. 25). The LREE enrichment is explained by the dominance of allanite and apatite over zircon.

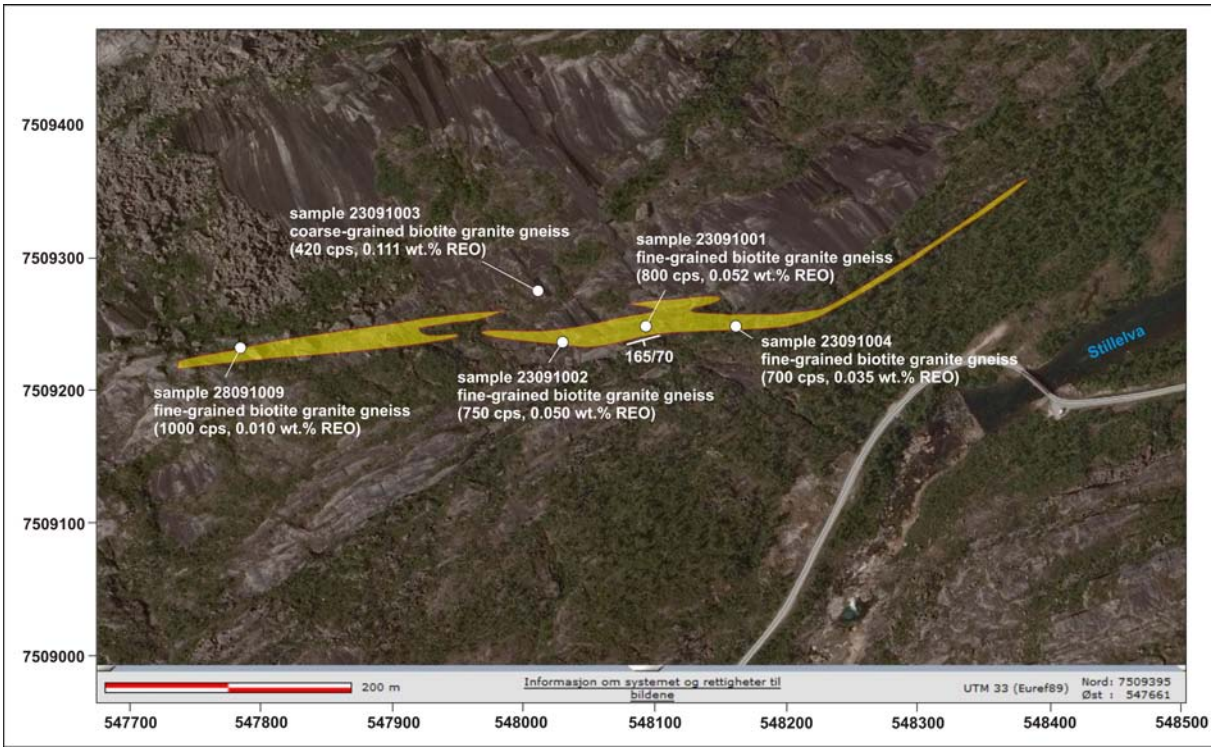

Figure 21. *Extension of the mineralised fine-grained biotite granite gneiss (yellow) north of Gjerdalsvatn with sample locations. The fine-grained gneiss forms a dyke in coarse-grained granite gneiss. Source of the air photograph: http://www.norgeibilder.no.*

Figure 22. *a – The mineralised granite gneiss dyke at Gjerdalsvatn in the foreground (bordered by the red dashed line) with view towards west to the Reinoksfjellet. b – Mineralised, fine-grained biotite granite gneiss from Gjerdalsvatn.*

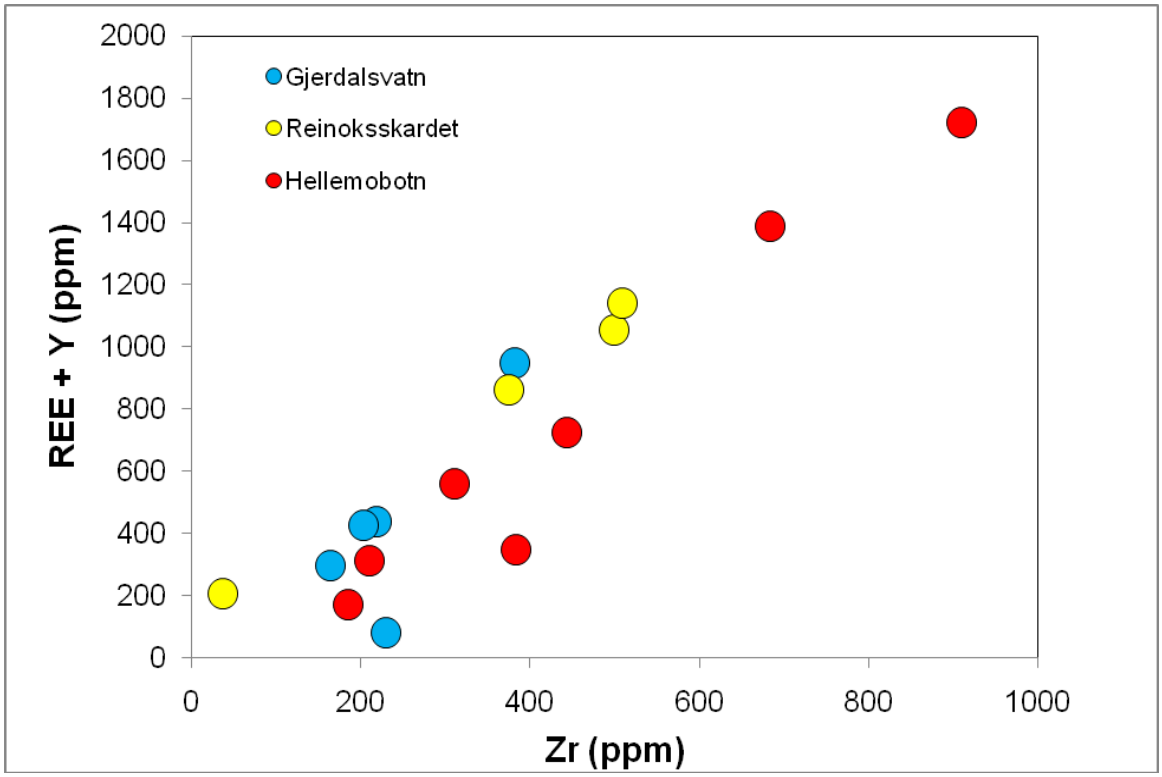

Figure 23. *Concentrations of Zr versus REE + Y of biotite granite gneisses from the central Tysfjord window.*

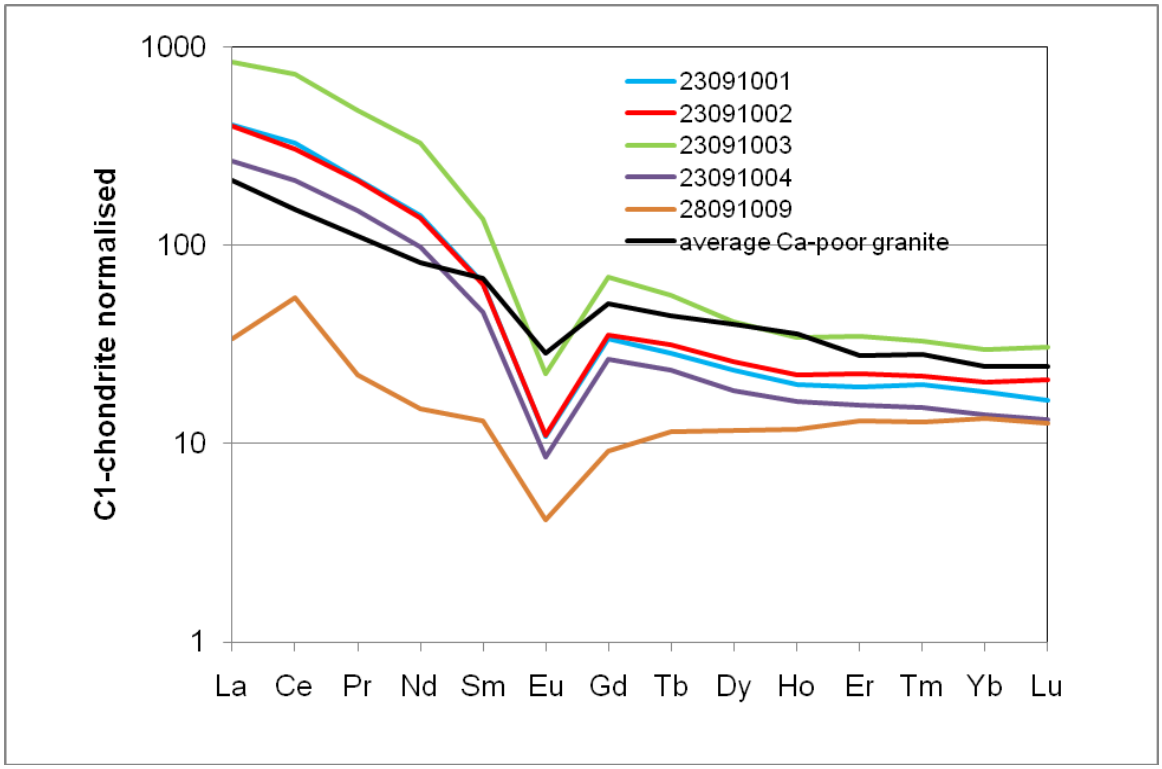

Figure 24. *Chondrite-normalised REE pattern of the Gjerdalsvatn samples compared with the pattern of average Ca-poor granites modified after Turekian and Wedepohl (1961).*

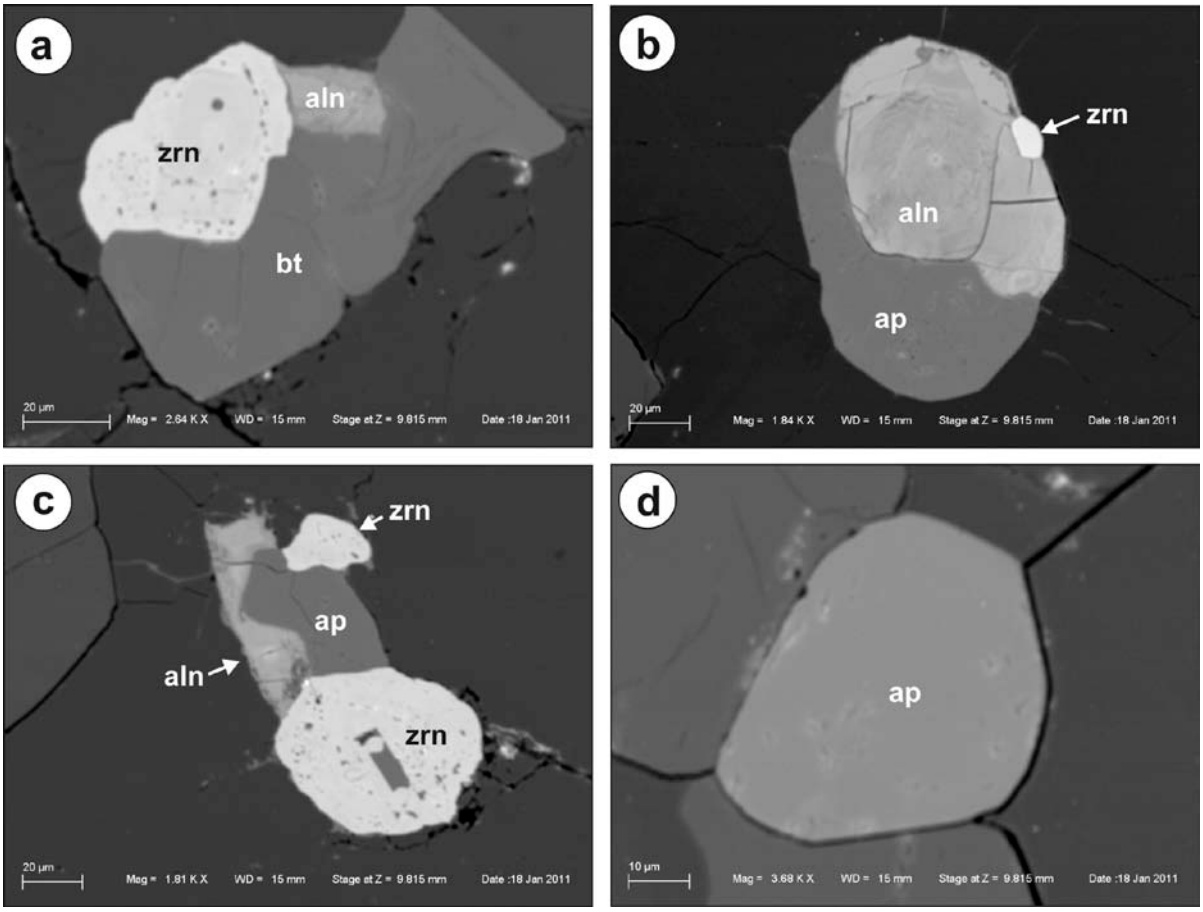

Figure 25. *BSE images of accessory REE-bearing minerals in the Gjerdalsvatn granite gneiss. a – Intergrowth of biotite (bt), zircon (zrn) and allanite (aln). b - Intergrowth of apatite (ap), allanite (aln), and zircon (zrn). c – Intergrowth of allanite (aln), apatite (ap), and zircon (zrn). d – Subhedral, homogeneous apatite crystal.*

5.2 Reinoksskardet

The target area north of Reinoksvatn was suggested in NGU report 2010.037 due to several distinct Th-radiation anomalies (Müller 2010). Because of the limited time in the field and the difficult accessibility of the area, the sampling was restricted to the Reinoksskardet at the western end of the Reinoksvatn anomaly (Fig. 26). Three representative, coarse-grained biotite granite gneiss samples (23091007, -08, -09) and one granite gneiss sample (23091005) from the contact with a granitic pegmatite were collected (Fig. 27). The latter had a gamma-ray intensity of 1400 cps. Samples 23091007 - 09 are characterized by elevated REO+Y_2O_3 of 0.101 to 0.134 wt.%, Zr of 374 to 509 ppm and Th of 32 to 41 ppm (Fig. 23). REE are enriched compared to average granite but with a pronounced negative Eu anomaly (Fig. 28). Sample 23091005 has low REO+Y_2O_3 of 0.025 wt.% and Zr of 37 ppm but is enriched in U (26 ppm) explaining the high gamma-radiation. The sample is strongly depleted in LREE probably due to the leaching of allanite and apatite in the granite gneiss near the pegmatite contact (Fig. 28). The most common accessory REE-bearing minerals are allanite (20-250 µm), apatite (20-60 µm) and zircon (20-120 µm) (Fig. 29). Very common allanite is responsible for the strong LREE enrichment. Secondary thorite and uraninite occur as alteration products of allanite (Fig. 29a).

Figure 26. *Hiking trail (red dashed line) and sampling locations at Reinoksskardet. The road leads towards the west to the dam at Reinoksvatn but was closed at the time of the visit due to a fresh rock fall from the Juoksatjåhkkå. Source of the air photograph: http://www.norgeibilder.no.*

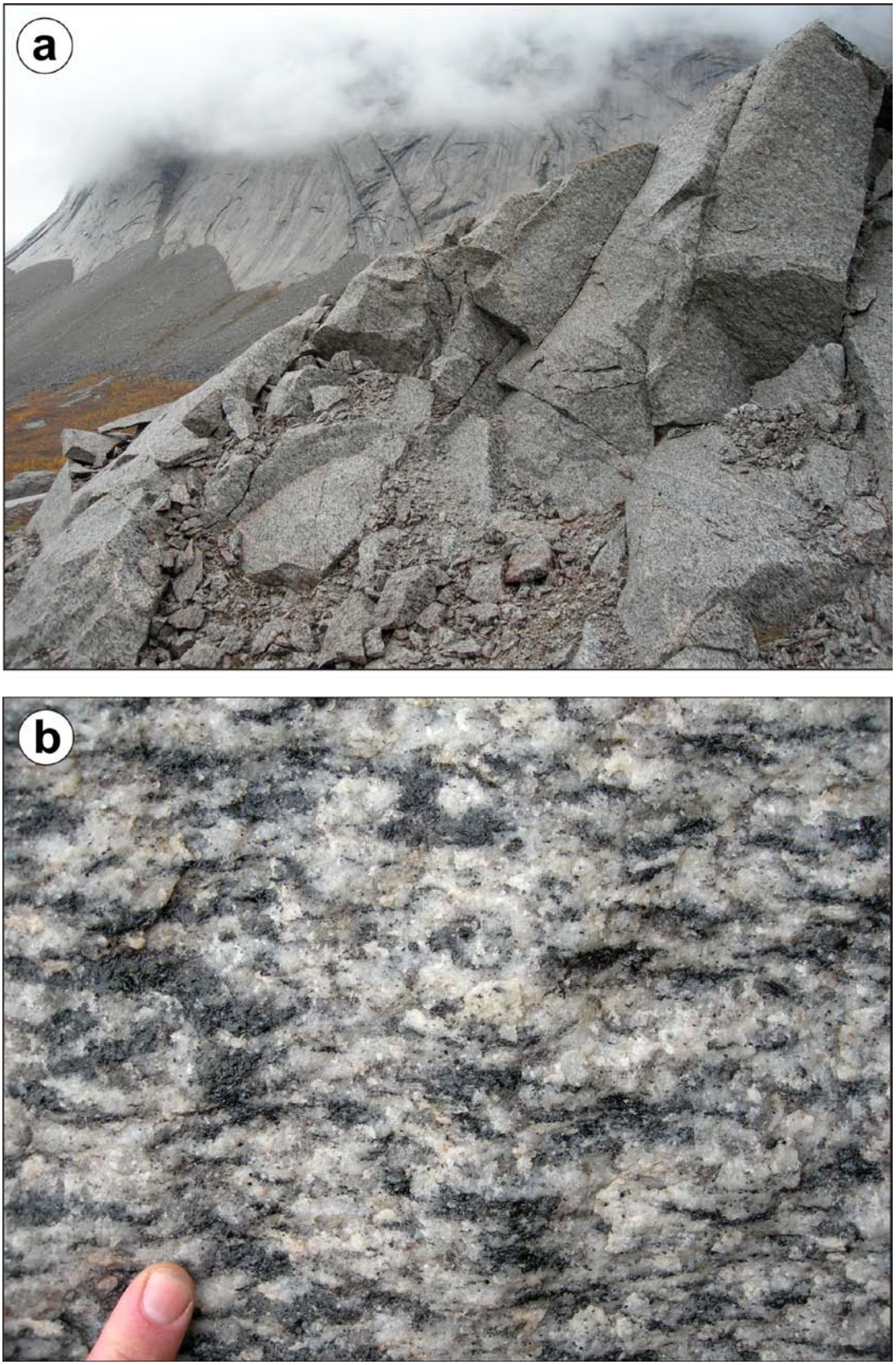

Figure 27. *a – Sampling location 23091008 with Reinoksfjellet in the background. b – Coarse-grained biotite granite gneiss at sampling location 23091008.*

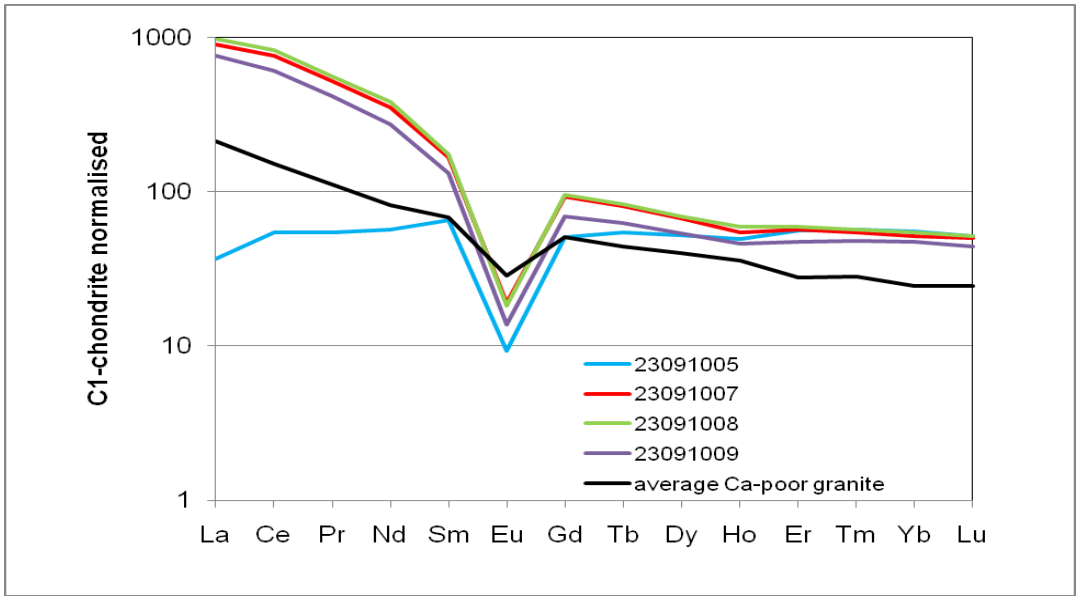

Figure 28. *Chondrite-normalised REE pattern of the Reinoksskardet samples compared with the pattern of average Ca-poor granites modified after Turekian and Wedepohl (1961). Sample 23091005, originating from the contact to granitic pegmatite, is depleted in LREE despite a high gamma-ray intensity of 1400 cps.*

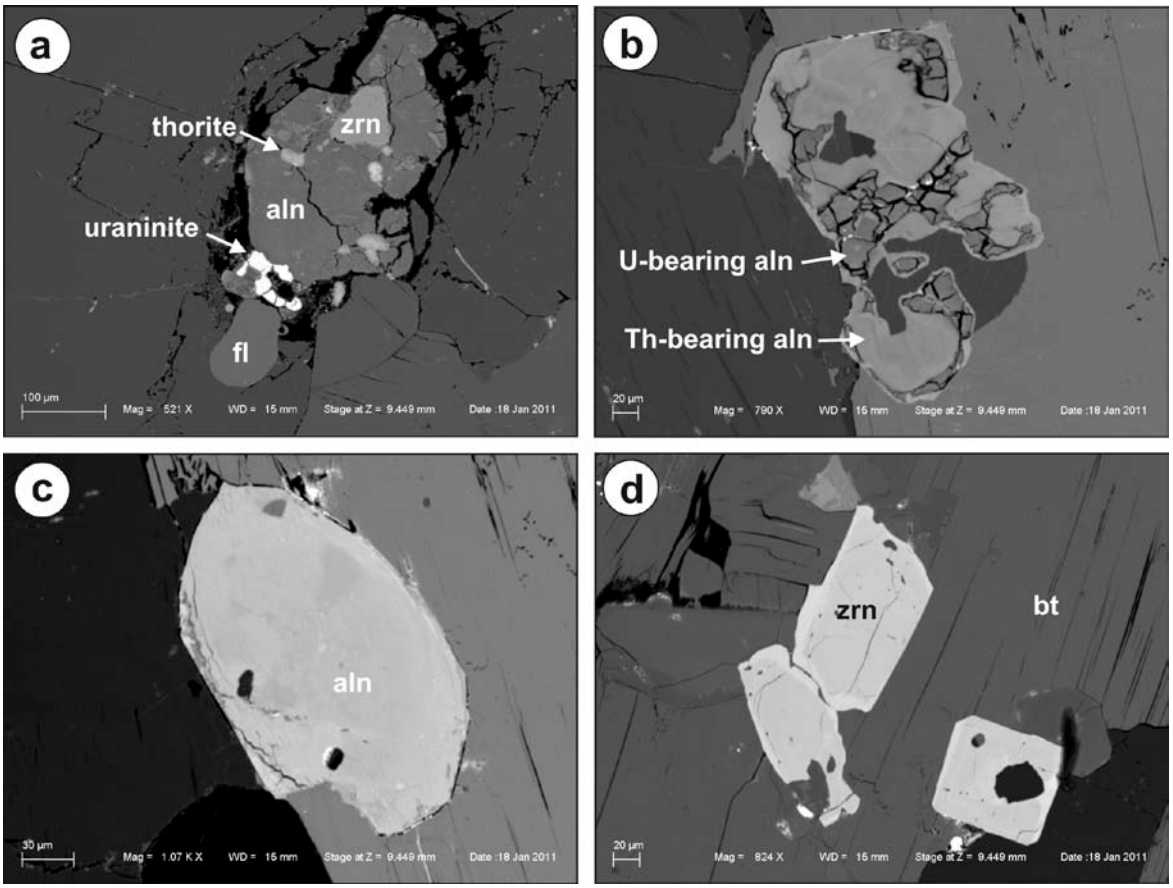

Figure 29. *BSE images of accessory REE-bearing minerals in the Reinoksskardet granite gneiss. a – Cluster of accessory minerals comprising allanite (aln), zircon (zrn), thorite, uraninite and fluorite (fl). b – Large allanite crystal with U-rich and Th-rich domains. c – Euhedral allanite (aln) crystal. d – Cluster of euhedral zircon crystals (zrn) surrounded by allanite, apatite and biotite (bt).*

5.3 Hellemobotn

Romer et al. (1992) provided a geochemical data set from the Hellemobotn granite gneisses. Four of the analyses showed unusually high REE-Th-U concentrations (Müller 2010). The samples originated from Amásvágge, ca. 4 km SE of Hellemobotn and were collected by A. Korneliussen and T. Grenne (NGU) in 1988. Figure 30 shows the route and sampling locations of the author following the route of Korneliussen and Grenne. The area is characterised by a high variability of gneiss textures including fine-, medium- and coarse-grained and porphyritic varieties. The background gamma-ray intensity is relatively high for all granite varieties, ranging from 500 to 900 cps. The gamma-ray anomaly was identified at 33V 566560/7520281 (sample 25091004) exactly at the site where A. Korneliussen and T. Grenne took the samples with high REE concentrations (Fig. 30b). The mineralised granite gneiss forms a NNW-striking, dyke-like structure which is 30 m wide. Due to the limited time the dyke could be followed for 300 m but it is presumably much longer. The mineralisation comprises et least 600 000 t assuming a minimum length of 300 m, a width of 30 m and a vertical extension of about 25 m. The ground-measured anomaly coincides with a small airborne-measured Th-radiation anomaly (Fig. 31). The anomaly lies on a NNW-NW striking structure which extends from the Swedish border to Vuodnabattjåhkkå, interrupted by the Ávttje canyon (Fig. 31).

Three samples (25091001 to -03) were collected from the high gamma-radiation area (>1000 cps) which forms a dyke-like structure consisting of medium-grained biotite granite gneiss. In addition, four different textural types of granite gneiss (samples 25091004 to -07) with gamma-ray signals from 500 - 900 cps were sampled (Fig. 30b). The highly radioactive samples contain 0.085 to 0.203 wt.% REO+Y_2O_3, the highest values reported in this project (Fig. 23). Zr concentrations range from 443 to 909 ppm, Th from 91 to 138 ppm and U from 20 to 33 ppm. The concentrations of the less radioactive granite gneisses are 0.018 to 0.038 wt.% REO+Y_2O_3, 185 to 383 ppm Zr, 23 to 70 ppm Th, 4 to 18 ppm U. In the case of the Hellemobotn granite gneisses, the gamma-ray radiation intensity correlates with REE-Th-U content. The highly radioactive samples are enriched in LREE and HREE compared to average granite (Fig. 32).

Titanite is the most common accessory mineral in the highly radioactive samples, with grain sizes of 40 to 2000 µm (Fig. 33; Table 1). The REE concentrations of titanite are low, <1%, but it is, nevertheless, considered as an important carrier of the LREE because of the its high abundance. Th-rich allanite occurs as inclusions in titanite and it seems that titanite replaced allanite (Fig. 33a). Allanite is the major accessory mineral in the less radioactive samples. Other common accessories are zircon (20-160 µm), apatite (20-60 µm) and magnetite (40-1000 µm). Less common accessories are fluorite (20-200 µm), polycrase-(Y) (5-10 mm) and thorianite (5-10 µm). Sample 25091006 contains large ilmenite crystals with exsolution structures.

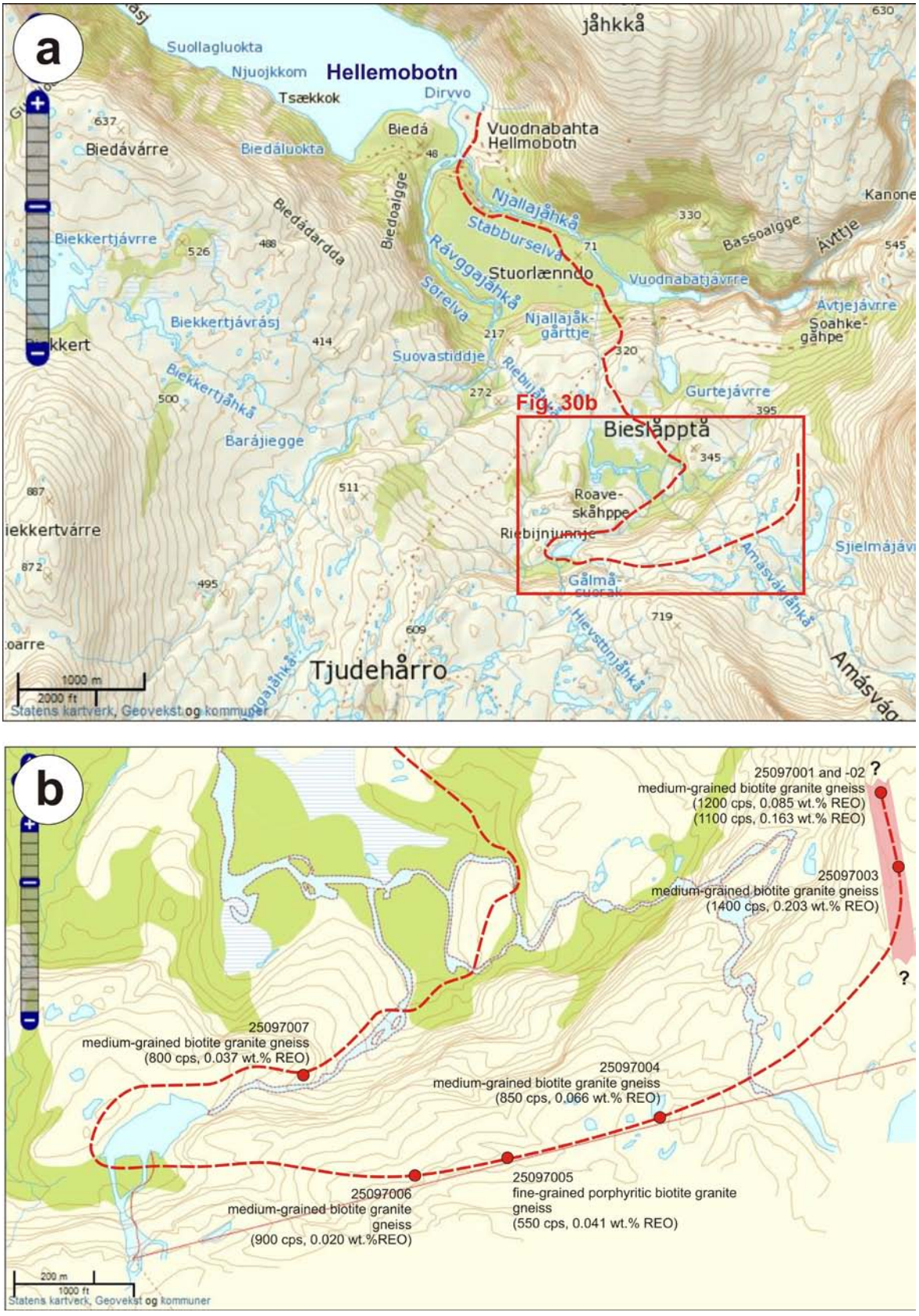

Figure 30. *Hiking trail (red dashed line) and sampling points south of Hellemobotn. Source of the air photograph: http://www.norgeibilder.no.*

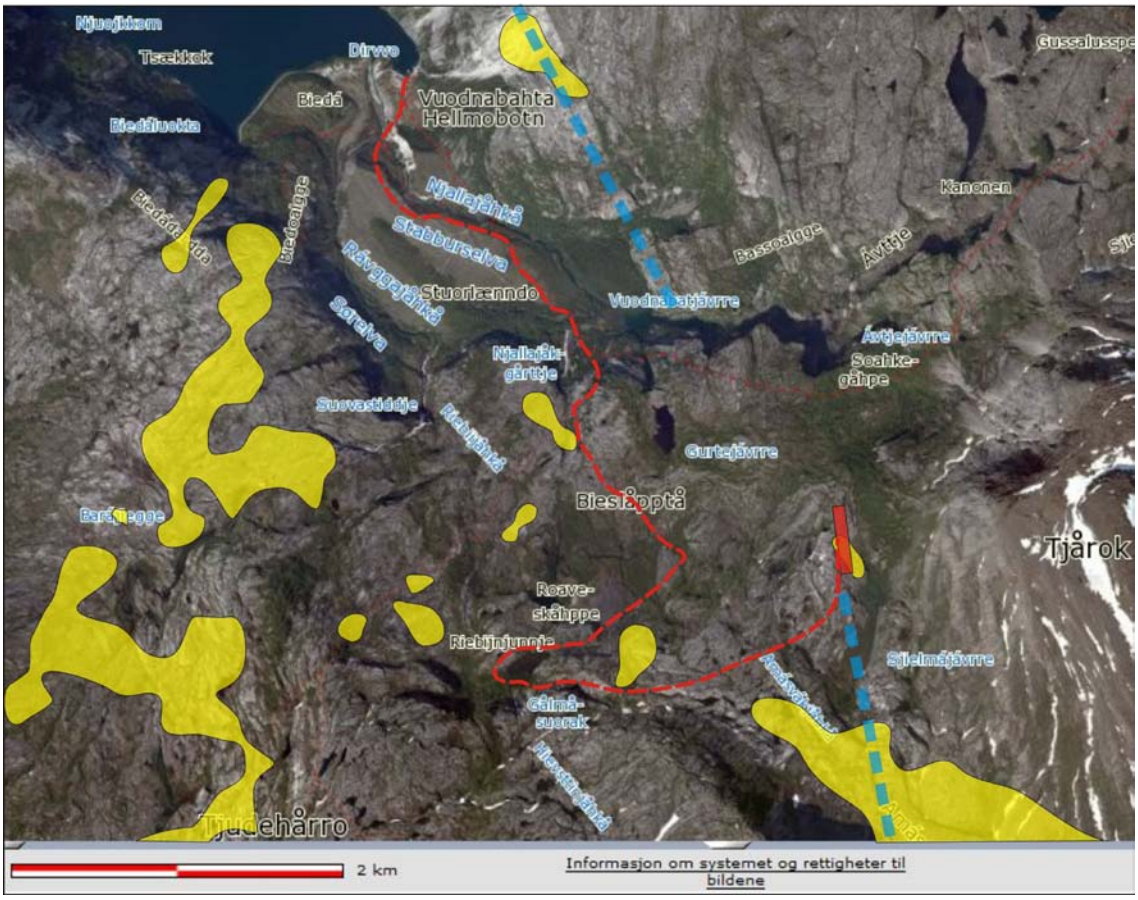

Figure 31. *Air photograph of the Hellemobotn area (source: http://www.norgeibilder.no) with airborne-measured Th-radiation anomalies (yellow; Th >130 cps), hiking trail (red dashed line), mineralised dyke (red bar) and major NNW-NW striking structures (blue dashed lines). Not that the mineralised dyke coincides with a small radiation anomaly.*

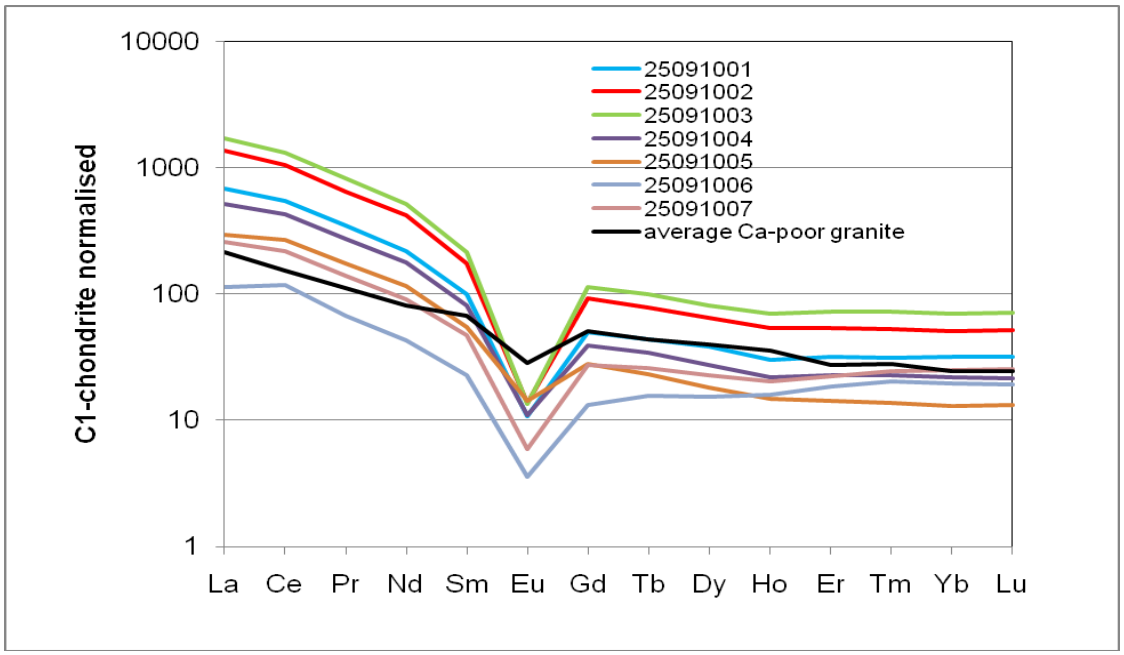

Figure 32. *Chondrite-normalised REE pattern of the Hellemobotn samples compared with the pattern of average Ca-poor granites modified after Turekian and Wedepohl (1961).*

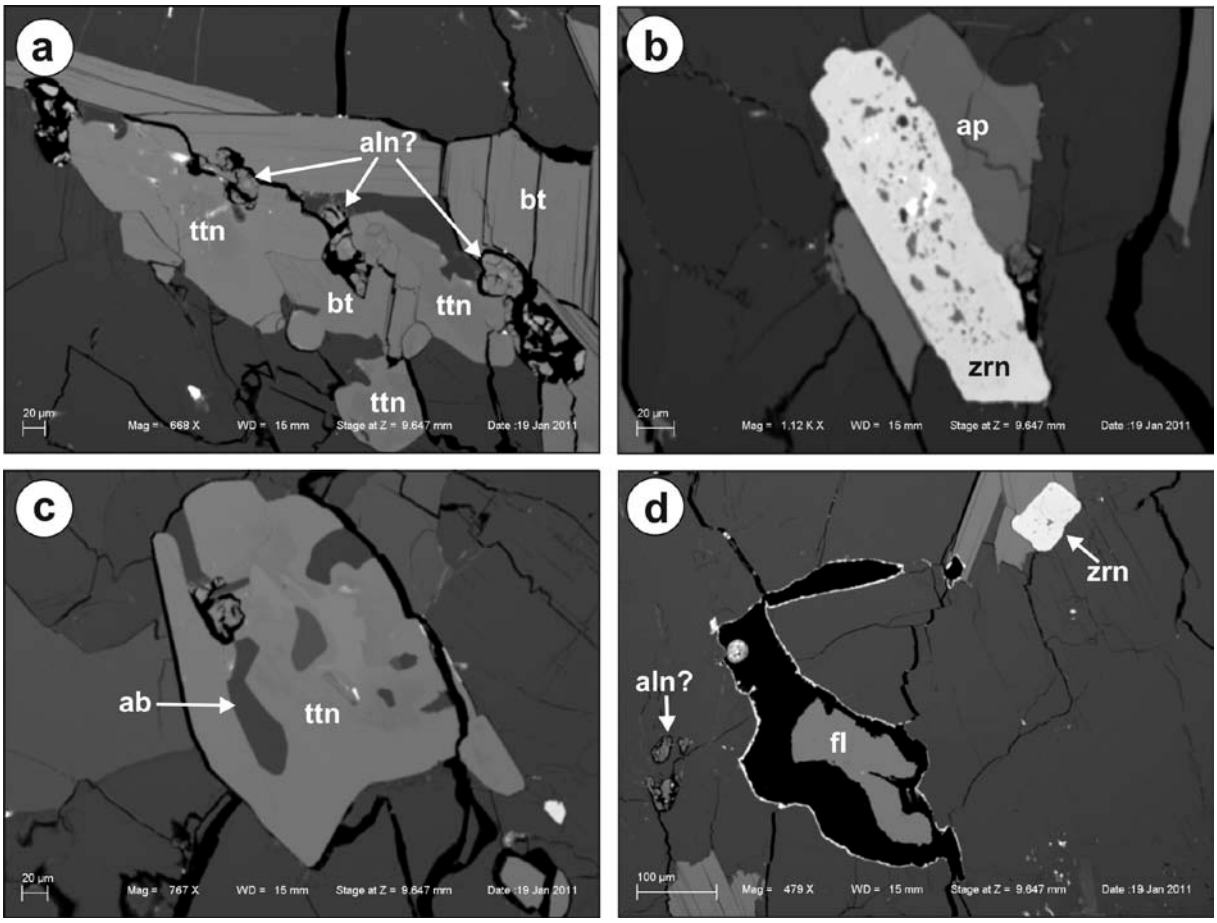

Figure 33. *BSE images of accessory REE-bearing minerals in the mineralised Hellemobotn granite gneiss. a – Cluster of biotite (bt) and titanite (ttn) with remains of allanite-like minerals (aln?) with high Th of up to 7 wt.% and no Ca. b – Porous zircon (zrn) overgrown by apatite (ap). c – Titanite crystal (ttn) with albite inclusions (ab). d – Corroded fluorite (fl) together with zircon (zrn) and small allanite-like crystals (aln?).*

5.4 Lagmannsvik pegmatite

The Lagmannsvik pegmatite is a granitic pegmatite situated on the central west border of the Tysfjord window. Because of the easy accessibility it was visited on the way to the northern Tysfjord area. The pegmatite forms a flat-lying, 80 m long and 30 wide lens which plunges 10 to 20º towards the WSW (Fig. 34). It consists of deformed K-feldspar, quartz and biotite, and minor plagioclase and muscovite. Common REE-bearing accessory minerals are allanite-(Ce), bastnäsite-(Ce), fluorapatite, yttrofluorite, gadolinite-(Y), monazite-(Ce) and thalénite-(Y). Scintillometer measurements detected high gamma-radiation, up to 40000 cps, in the central, basal part of the pegmatite body (marked with red dots in Fig. 34; Fig. 35). Massive REE-Th-U ore (up to 10 cm) occurs as brownish veins in K-feldspar in the high-radiation zones. SEM examination revealed that the massive REE-Th-U ore consists predominantly of zircon, thorite, allanite, apatite, xenotime-(Yb), monazite, thorite and cerphosphorhuttonite (Fig. 36). The mineralisation is too small (presumably <100 kg of massive ore) to be of economic interest. The chances to find similar mineralisations in the area are very low. However, another mined pegmatite which may be contains REE-Th-U mineralisations occurs about 250 m north of the Lagmannsvik pegmatite.

Figure 34. *Location of the Lagmannsvik pegmatite (light grey area) next to the E6 400 m north of the farm Lagmannsvik with Th-U-REE mineralisations (red dots).*

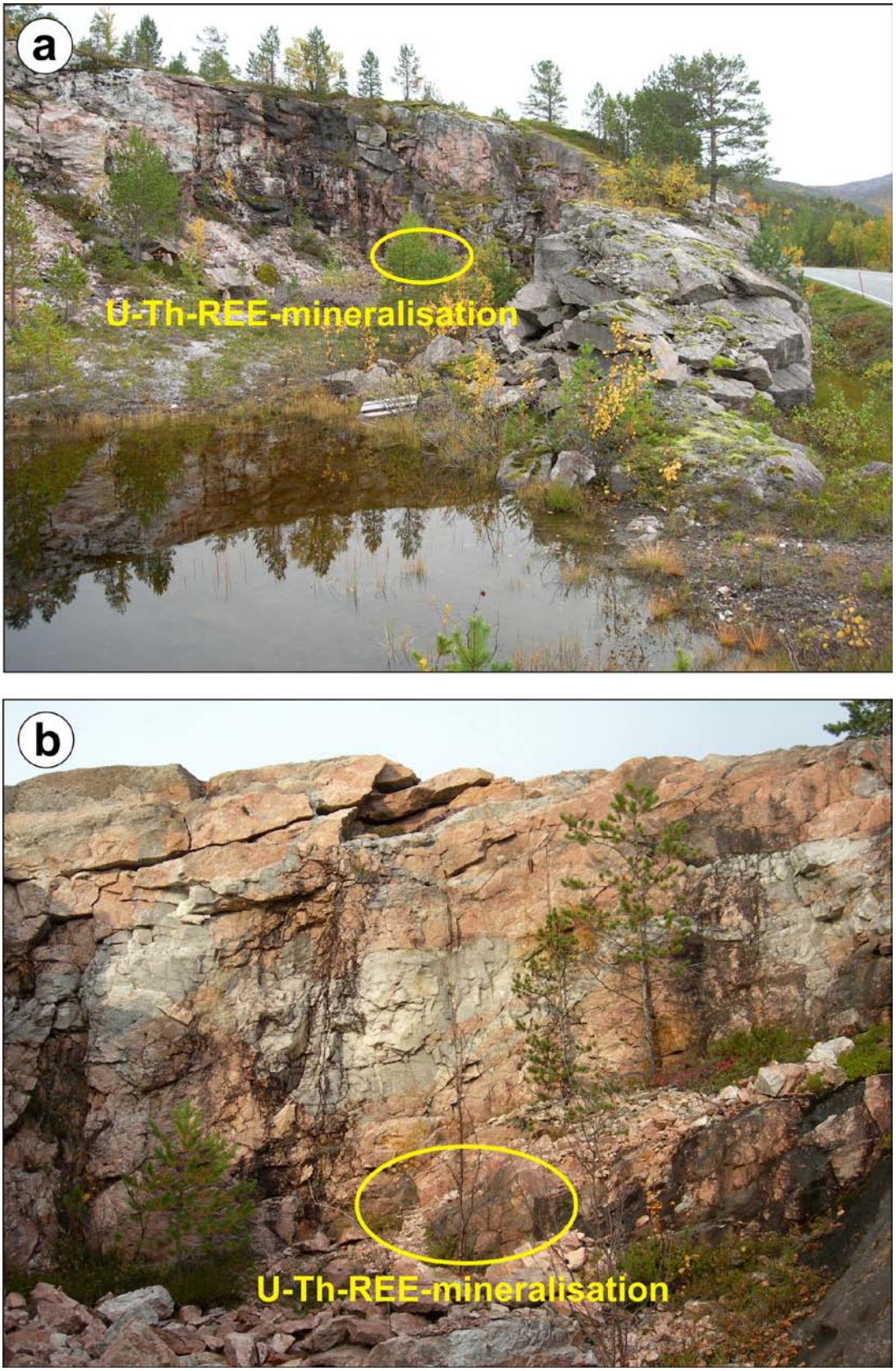

Figure 35. *a – Main pit of the Lagmannsvik pegmatite with location of the U-Th-REE mineralisation in the bottom of the southern wall. Quartz and K-feldspar megacrysts are deformed to flat-lying lenses. View towards south with the E6 on the right. b – Small southern pit with the location of the U-Th-REE in the bottom of the north wall. The pegmatite is ductile deformed.*

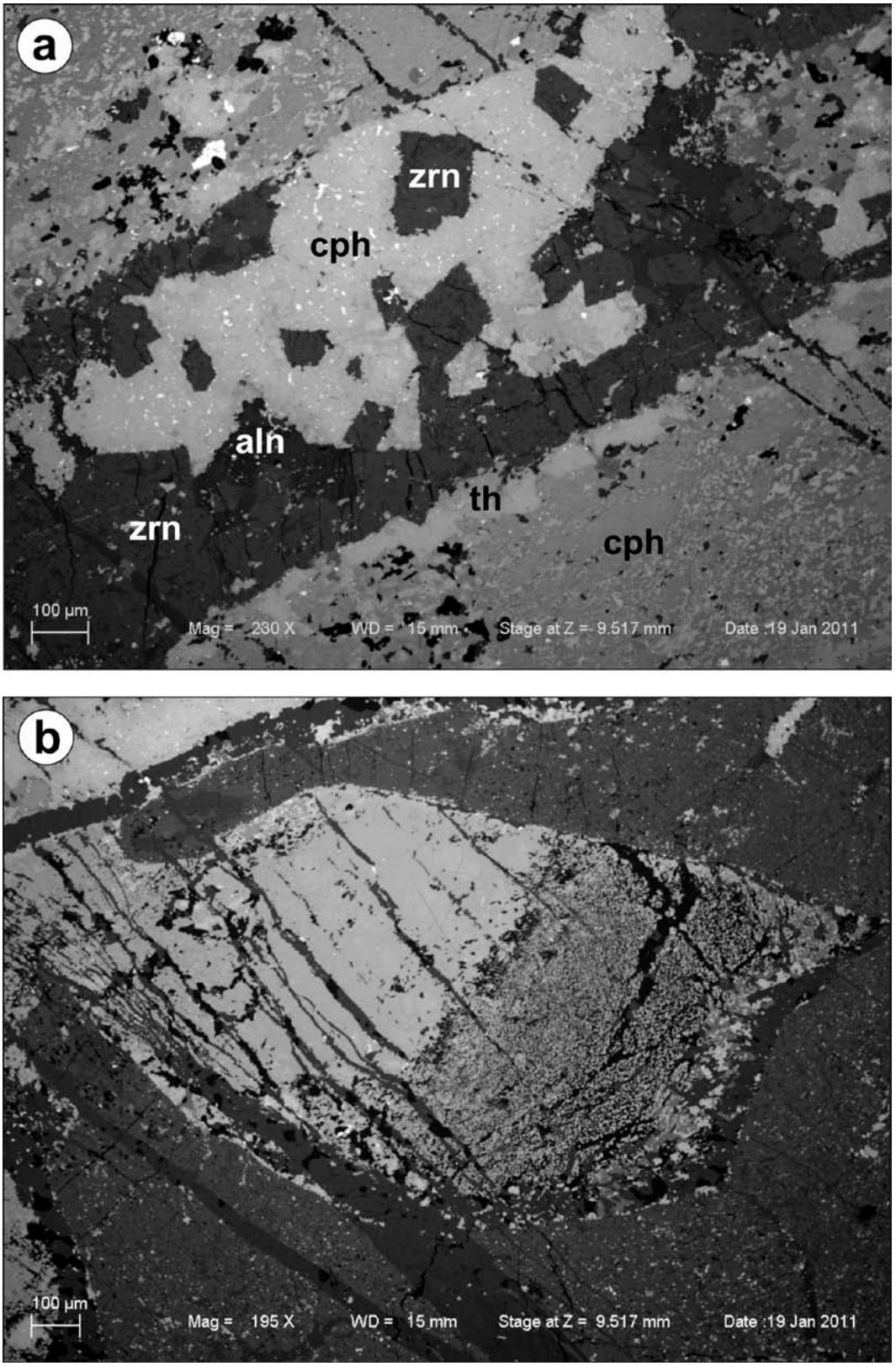

Figure 36. *BSE images of U-Th-REE ore of the Lagmannsvik pegmatite. a – Massive U-Th-REE ore comprising predominantly zircon (zrn), cerphosphorhuttonite (cph), thorite (th), and allanite (aln). b – Massive Th-REE ore comprising predominantly (from dark to bright minerals) apatite, allanite, zircon, xenotime-(Yb), monazite and thorite.*

6. Northern Tysfjord window

6.1 Hundholmen

The Hundholmen pegmatite is a granitic pegmatite which was mined from 1906 up to around 1970 for feldspar, some quartz and fluorite. The fluorite is enriched in Y and Ce in the form of yttrofluorite, cerfluorite and fluocerite (Husdal 2008). Common REE-Th-U minerals of the Hundholmen pegmatite are allanite, bastnäsite-(Ce), columbite-(Fe), euxenite-(Y), fluocerite-(Ce), fluorapatite, fluorite, fluorthalénite-(Y), fergusonite-(Y), gadolinite-(Y), hingganite-(Y), hundholmenite-(Y), monazite, synchysite, tengerite-(Y), thalénite-(Y), thorite, uraninite, xenotime, zircon. With respect to REE, Y, Th and U mineralisations the exploited pegmatite has no economic potential. However, the host granite of the Hundholmen pegmatite is described as grey, medium- to coarse-grained biotite-amphibole alkali granite with very common allanite and titanite (Vogt 1922). The amphibole is hastingsite – a Na-Ca amphibole. Whole-rock analyses of this granite are not reported. Due to its mineralogical description, the host granite of the Hundholmen pegmatite may have elevated REE concentration, therefore, the area was suggested as target area in the NGU report 2009.037.

The pegmatite and the Hundholmen area were visited together with Tore Vrålstad and Ola Torstensen, chief geologist of the Nordland county (Fig. 37). First, the waste heap of the former pegmatite mine was examined. Several large pieces of greenish white fluorite were found (Fig. 38). The fluorite can hardly be distinguished from quartz. The most distinguishing feature is the hardness. Semi-quantitative EDX analyses revealed that the fluorite contains less than 1 wt.% REE. However, the fluorite contains common inclusions of a Y-Ca-silicate which could not be identified (Fig. 39a). Less common are gadolinite inclusions which occur together with muscovite crystals in the fluorite (Fig. 39b).

The host, coarse-grained granite gneiss close to the pegmatite had very low gamma-ray intensity of 250 cps. In addition the rocks of the outcrop were weathered and leached by sea water. It was decided to take a fresh granite gneiss sample from a road cut about 2 km SE of the pegmatite (Fig. 37a). At the road cut (33V 0553636/7558054) the granite gneiss had a gamma radiation intensity of 550 cps. The analysis revealed 0.062 wt.% REO+Y_2O_3, 665 ppm Zr, 24 ppm Th and 7 ppm U (Fig. 40, Appendix 2). LREE and in particular HREE are enriched compared to average granite composition (Fig. 41). An interesting feature is the weaker Eu anomaly compared to the other Tysfjord granites. The reason for the strong HREE enrichment is the high abundance of zircon, reflected by the high Zr concentration. Because of the low radiation intensity, SEM examination was not carried out on the sample.

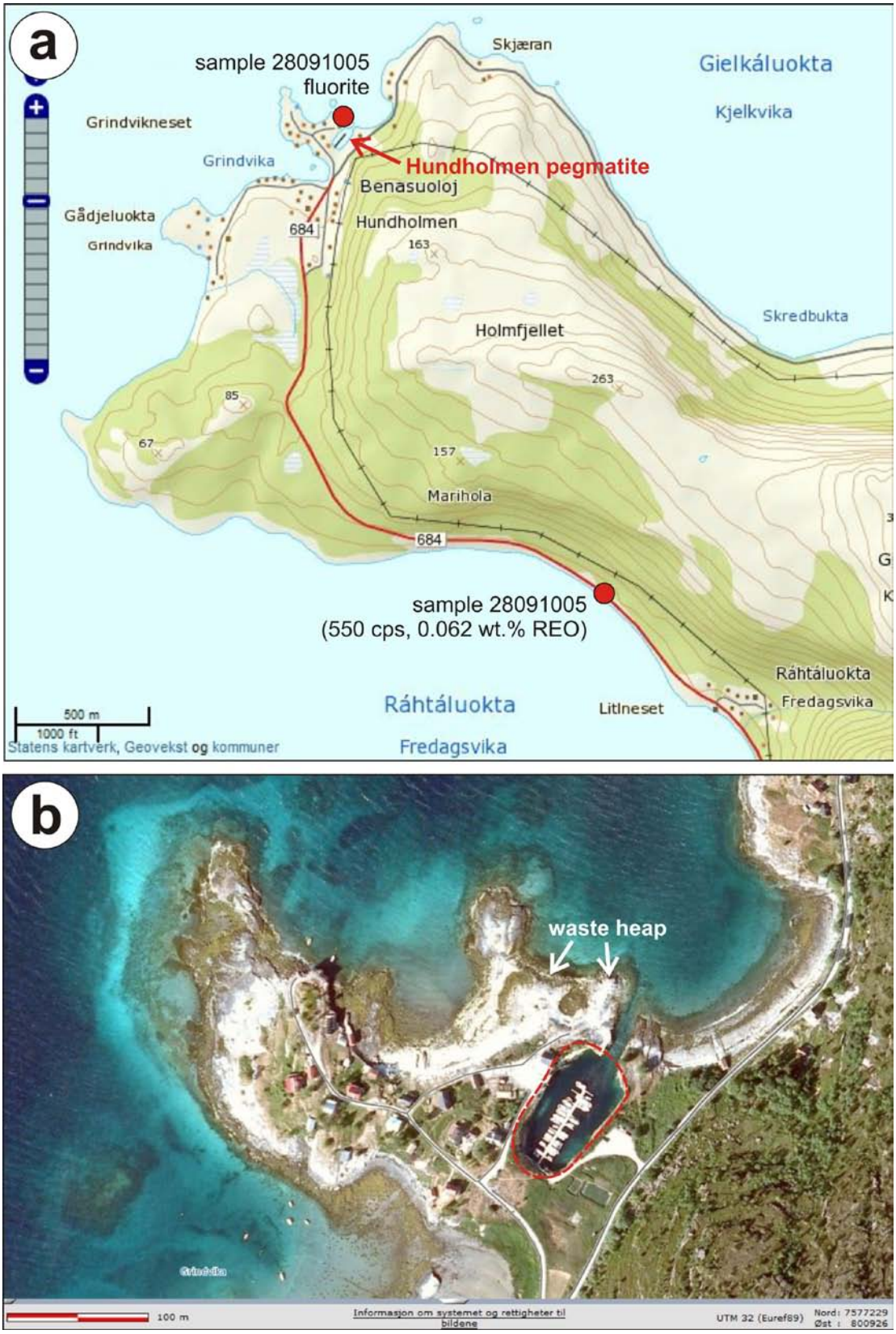

Figure 37. *a - Locations of the Hundholmen pegmatite and the sampling point of the Hundholmen granite gneiss. b – Air photograph of the Hundholmen pegmatite mine (red dashed line) which is today flooded and used as port for sailing boats. The fluorite sample was found on the waste heap of the former pegmatite mine.*

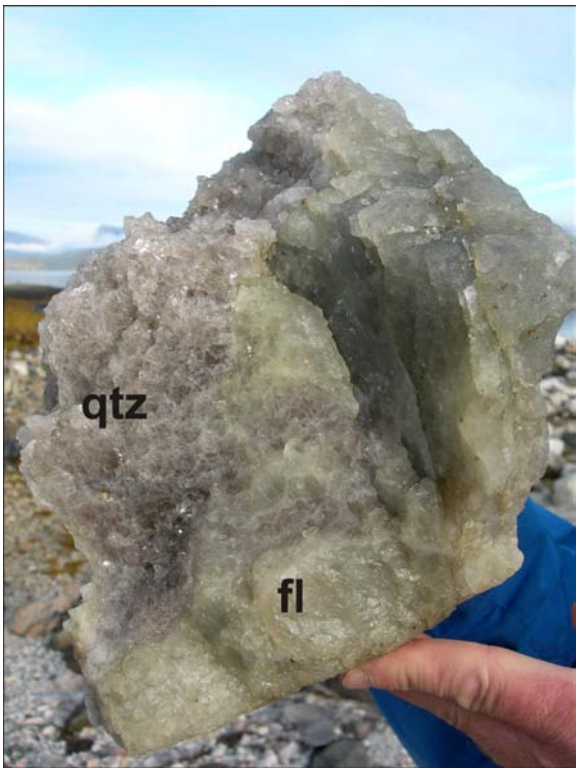

Figure 38. *Quartz (qtz) from the pegmatite core with greenish white fluorite (fl).*

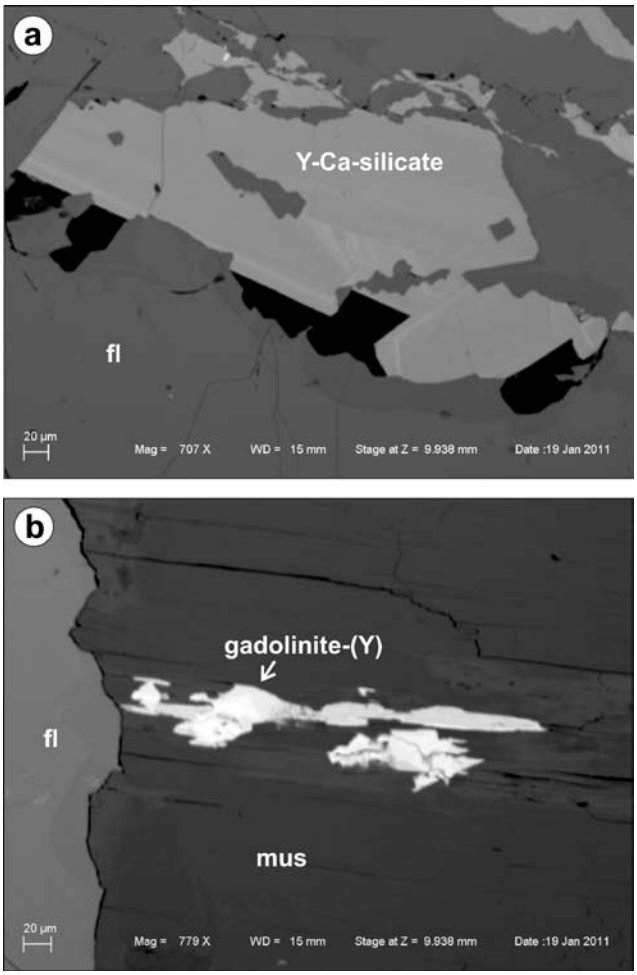

Figure 39. *BSE images of inclusions of REE-bearing minerals in fluorite from the Hundholmen pegmatite. a – Y-Ca-silicate which could be britholite-(Y) or gerenite-(Y). These type of inclusion in fluorite is very common. b – Gadolinite-(Y) and muscovite included in fluorite.*

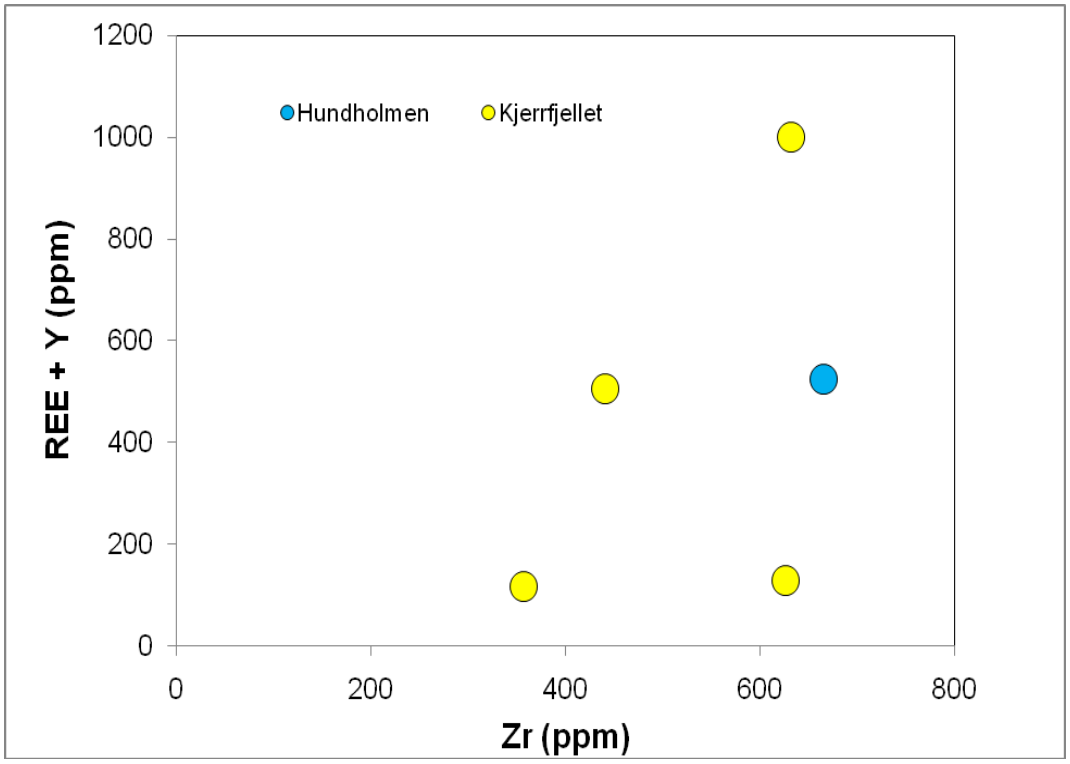

Figure 40. *Concentrations of Zr versus REE + Y of biotite granite gneisses from Hundholmen and Kjerrfellet. The mineralised granite gneisses have >500 ppm REE+Y.*

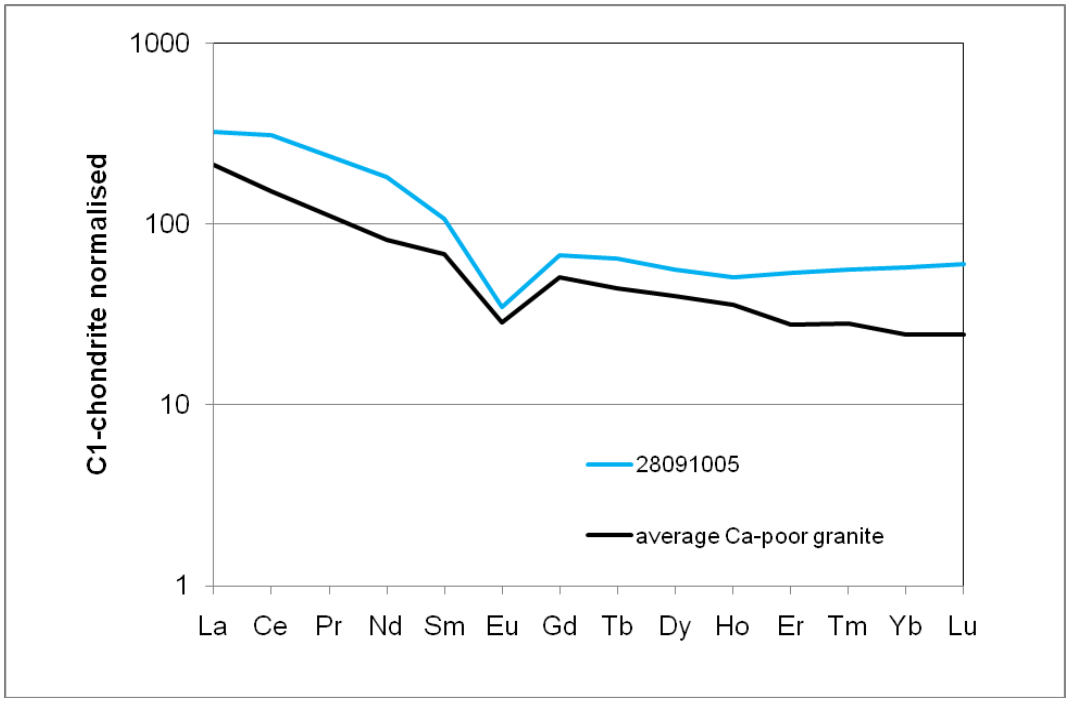

Figure 41. *Chondrite-normalised REE pattern of the Hundholmen granite gneiss compared with the pattern of average Ca-poor granites modified after Turekian and Wedepohl (1961).*

6.2 Kjerrfjellet

Several airborne-measured Th-radiation anomalies along the SW-NE striking Kjerrfjellet mountain ridge were the reason for the region being chosen as a target area. Figure 42 shows the radiation anomalies (yellow shaded areas), the hiking trail and sampling points. The TIB granite gneiss exposed along the hiking trail at Svarthammaren had a very low gamma-radiation intensity of 150 to 200 cps. Almost exactly where the anomaly was entered, the radiation intensity of the granite gneiss increased to 500 cps. Four samples of medium-grained granite gneiss were taken (Fig. 43). The samples have a highly variable REO+Y_2O_3 of 0.014 to 0.118 wt.% despite relatively consistent gamma-radiation signals (Figs. 40, 42). Only sample 24091004 show a strong enrichment of LREE and HREE compared to the average granite composition (Fig. 44). Samples 24091001 and -03 are strongly depleted in LREE probably due to the leaching of apatite during secondary overprint. Zr concentrations are 357 to 631 ppm, Th 14 to 40 ppm and U 3 to 8 ppm. The dominant accessory REE-bearing minerals are zircon (20-60 µm) and apatite (20-300 µm) (Fig. 45, Table 1). In addition almandine-like minerals with 1 wt.% P and Cl and 60 to 100 µm in size are common. The minerals form euhedral and zoned inclusions in biotite (Fig. 45b). Summarizing, the Kjerrfjellet granite gneiss has no potential for economic REE mineralisation. The airborne-measured Th-radiation anomalies along the Kjerrfellet mountain ridge are so distinct because of the low radiation signal of the surrounding granite gneiss.

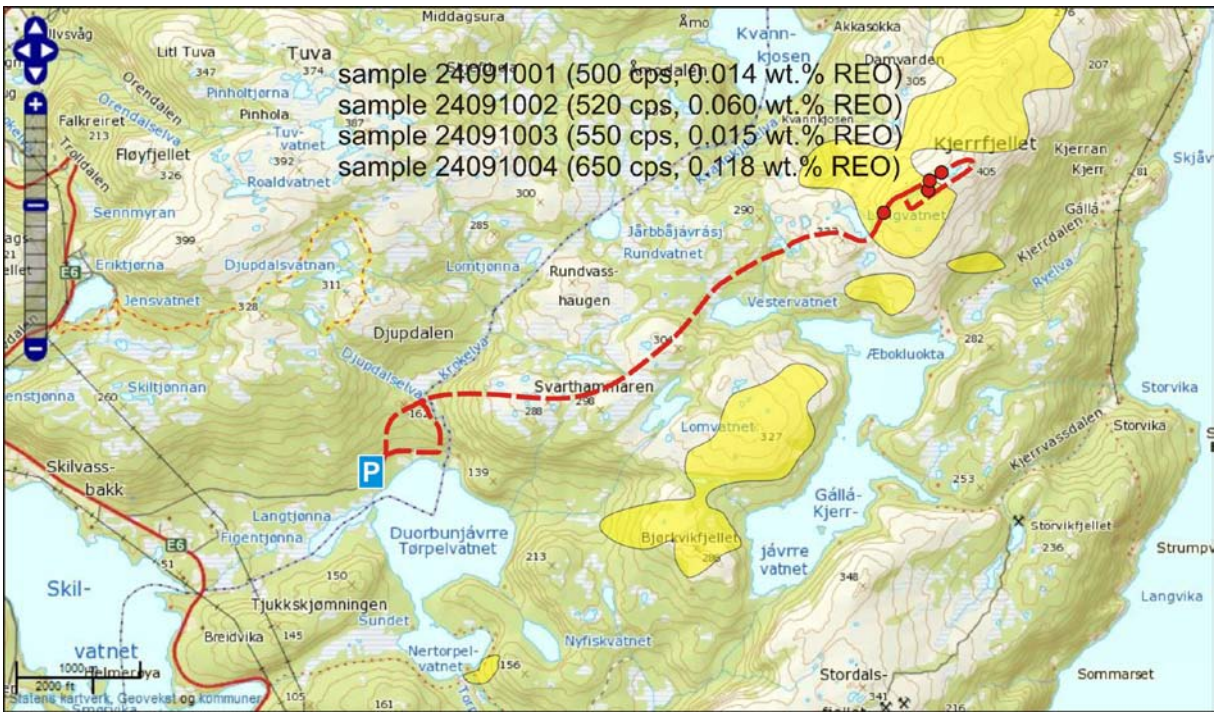

Figure 42. *Map of the Kjerrfjellet area with airborne-measured Th-radiation anomalies (yellow; Th >36 cps), hiking trail (red dashed line), and sampling points (red dots).*

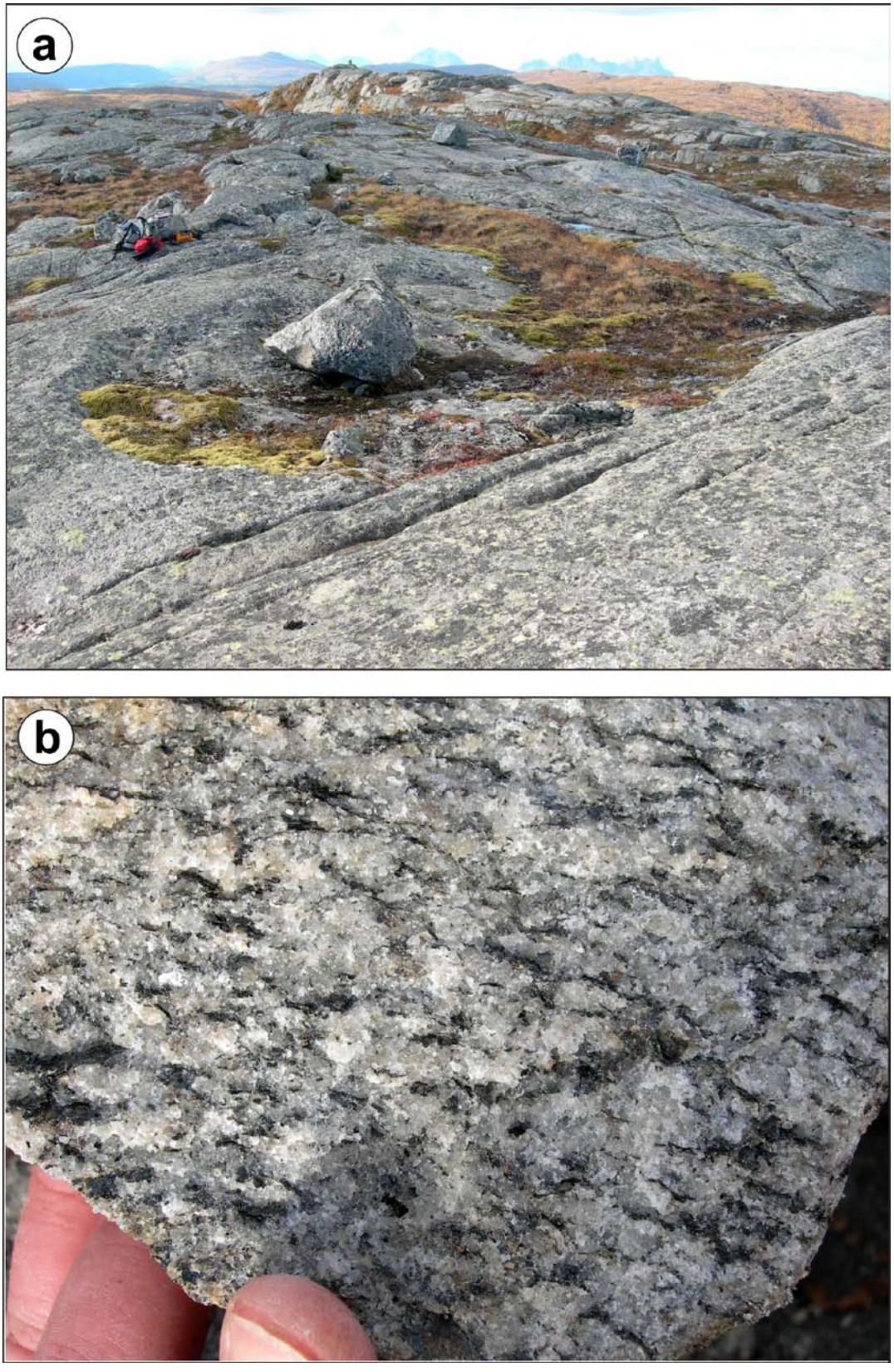

Figure 43. *a - Plateau of the Kjerrfjellet with sampling point 24091002 in the midground. View towards SW. b – Medium-grained biotite granite gneiss from Kjerrfjellet.*

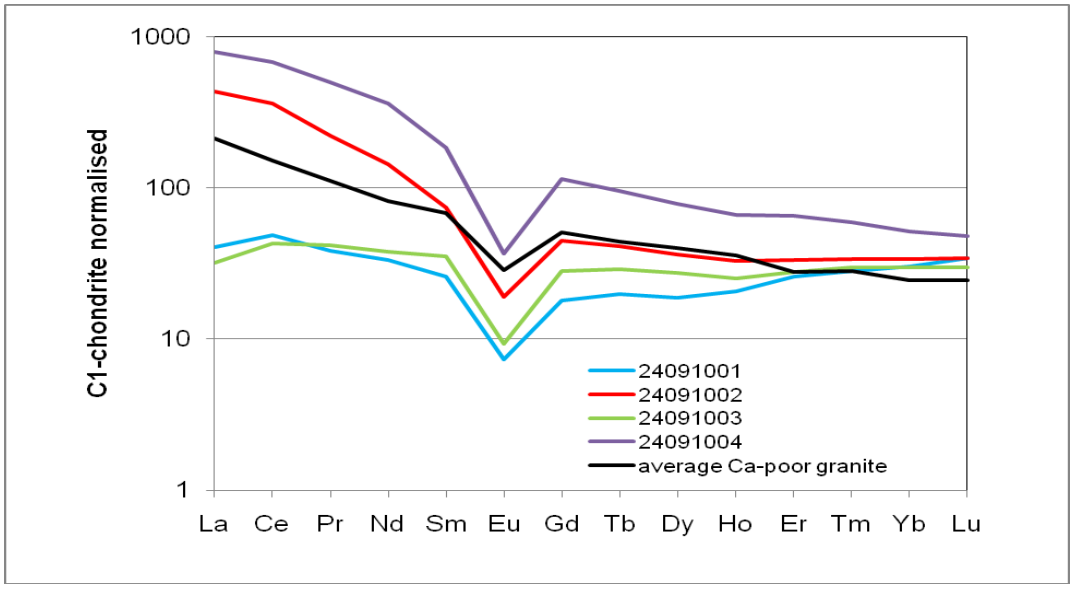

Figure 44. *Chondrite-normalised REE pattern of the Kjerrfjellet samples compared with the pattern of average Ca-poor granites modified after Turekian and Wedepohl (1961).*

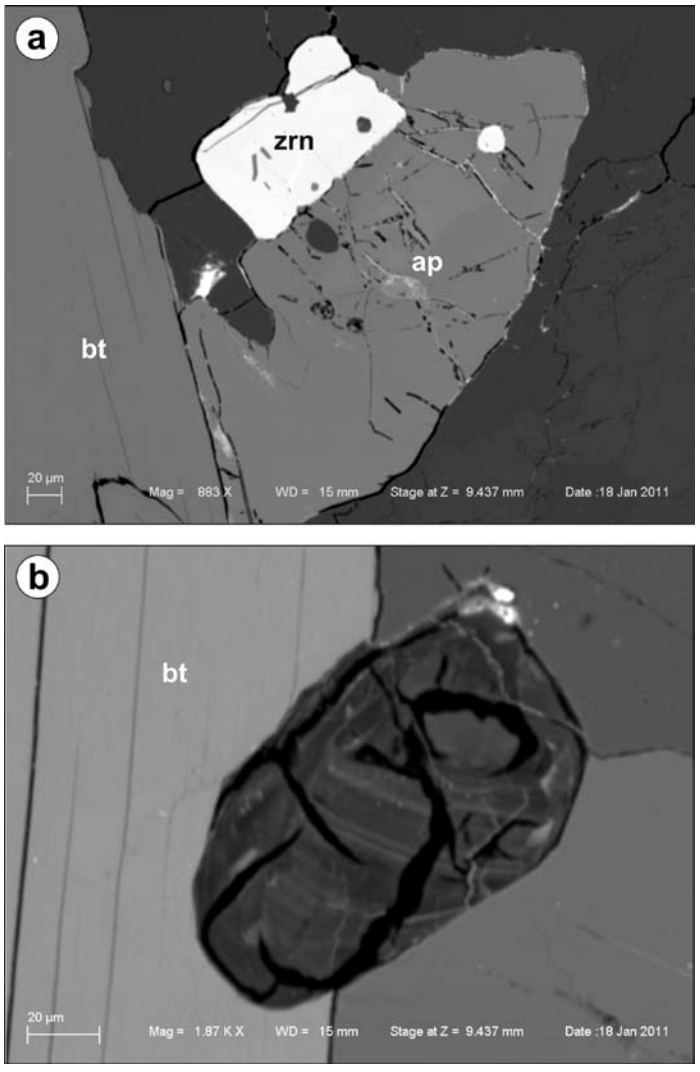

Figure 45. *BSE images of REE-bearing minerals in the Kjerrfjellet granite gneiss. a – apatite intergrown with zircon. Apatite is very common in the rock. b – Common accessory mineral of almandine composition with 1 wt.% P and 1 wt.% Cl.*

6.3 Hatten-Tilthornet massif

The Hatten-Tilthornet massif has been suggested as a investigation target due to several small distinct, airborne-measured Th-radiation anomalies (Fig. 46; Müller 2010). Two of the anomalies were visited during a 6-hour hiking tour, starting and ending at the highest point of the toll road Skardvikveien (Fig. 3). Fine- to coarse-grained biotite granite gneisses (TIB-type Tysfjord granites) with gamma-ray signals of 110-150 cps are exposed south of the Hundmulen mountain. Blocks of fine-grained biotite granite gneiss with a gamma-ray signal of 450 cps were found at 33V 0538322/7562471. The blocks originate from the top of the Hundholmen mountain and are thus from the area of the airborne-measured radiation anomaly. Fine-grained biotite granite gneisses exposed within the areas of the airborne-measured radiation anomalies at Storskartinden and south of the Hatten mountain had gamma-ray intensities of 280 to 300 cps. Because of the low gamma-ray signals of the rock, no samples were taken from the area. There seems to be no potential for economic REE-mineralisations in the area.

On the western flank of the Hundmulen mountain a small old haematite skarn mine is situated (Figs. 46, 47). The skarn mineralization is hosted by calc-silicate gneisses, being part of a metamorphosed sedimentary and volcanic supracrustal sequence.

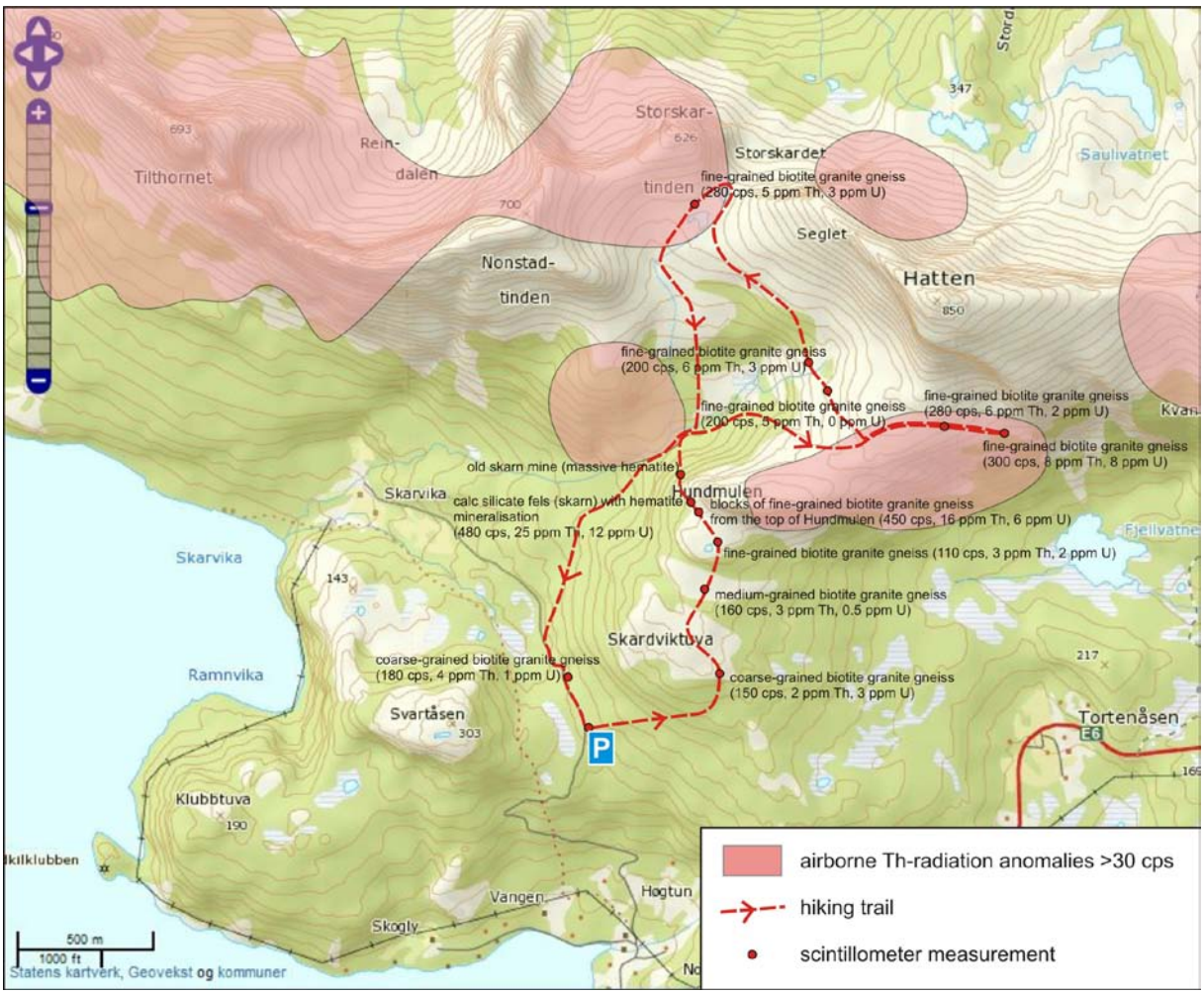

Figure 46. *Topographic map of the Tilthornet-Hatten massif with airborne Th-radiation anomalies, hiking trail and scintillometer measurements.*

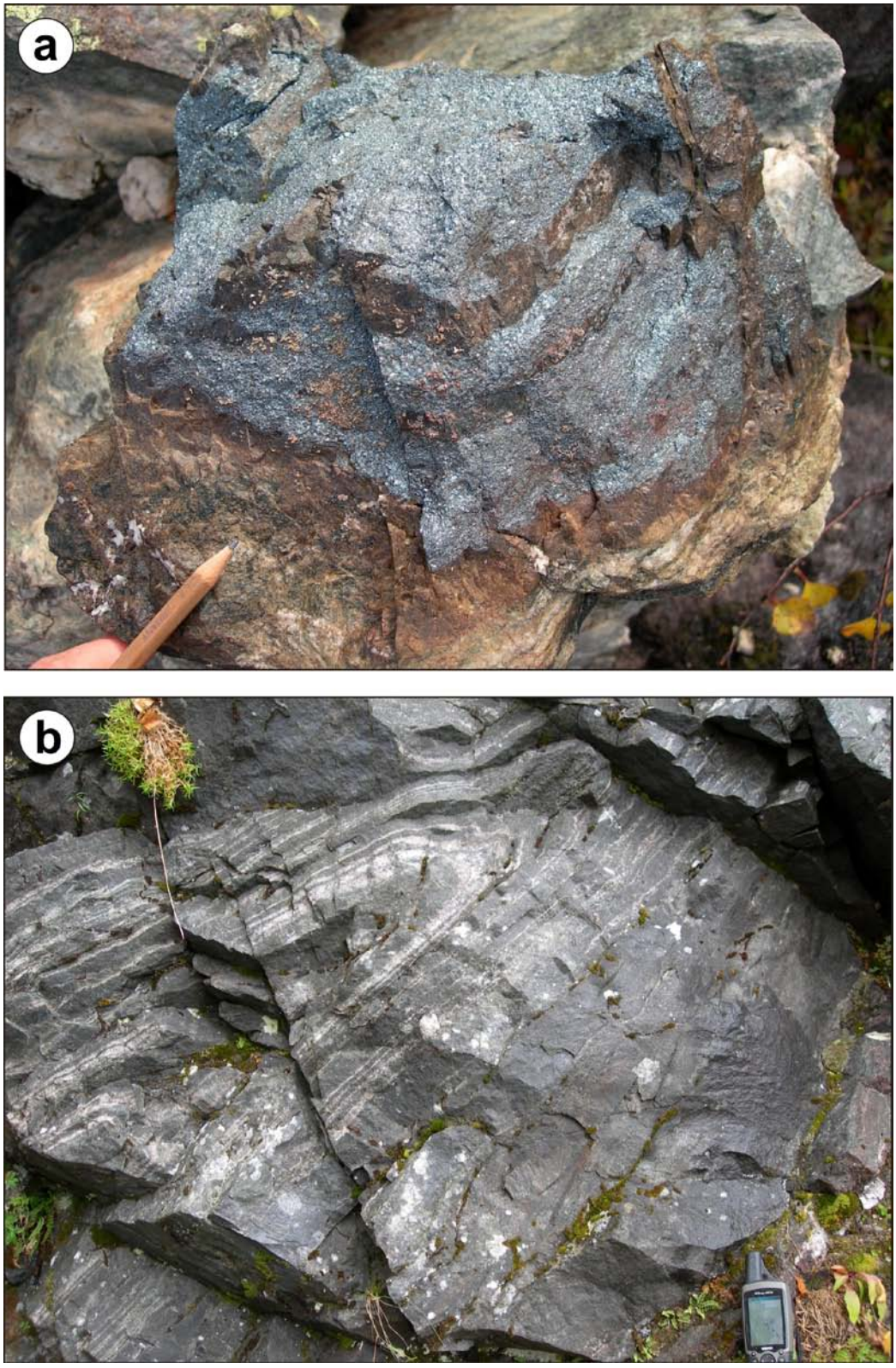

Figure 47. *a – Block of haematite skarn from the top of the Hundmulen mountain. b – Small, old mine in massive haematite skarn at 33V 0538352/7562584.*

7. Summary and outlook

During the field campaign which was carried out in September 2010, the target areas of potential REE-Zr mineralisations suggested in the NGU report 2009.037 (Müller 2010) were examined and sampled. The airborne-measured Th-radiation anomalies situated in the target areas were identified by applying gamma-ray scintillometer measurements. The rocks of the target areas comprise evolved Proterozoic TIB-2-type granite gneisses (1719-1703 Ma; Romer et al. 1992) of the Rishaugfjell, Sommerset and Tysfjord basement windows. The rocks are subalkaline, metaluminous and deformed granites (granite gneiss) with A-type (anorogenic) affinity enriched in REE and Zr (Müller 2010).

Table 2. REO+Y_2O_3 concentrations, common accessory minerals and tonnage of TIB granite gneisses which cause gamma-ray anomalies in the Tysfjord area.

	REO+Y_2O_3 (wt.%) (nr. of representative analyses)	**Tonnage**	**Gamma-ray signal** (ground-measured)	**REE-bearing accessory minerals**
Memaurvatn	0.067 (3)	300 000 t	1400	allanite, zircon fluorite
Sommerset	0.064 (2)	>100 Mt	700	allanite, zircon, apatite, titanite, synchysite
Rismålsvatn	0.057 (2)	>100 Mt	500	not determined
Gjerdalsvatn	0.052 (5)	150 000 t	800	allanite, zircon, apatite
Reinoksskardet	0.120 (3)	>100 Mt	650	allanite, zircon, apatite
Kjerrfjellet	0.030 (3)	10 Mt	500	zircon, apatite
Hellemobotn	0.150 (3)	600 000 t	1200	allanite, zircon, apatite, titanite
Hundholmen	0.062 (1)	>100 Mt	500	not determined

REO+Y_2O_3 concentrations of the TIB granite gneisses of the investigated target areas are listed in Table 2. The highest REO+Y_2O_3 concentrations have the granite gneisses at Hellemobotn and Reinoksskardet of 0.15 and 0. 12 wt.%, respectively (Fig. 48). The high REE-Zr-Th values of the mineralised Sommerset granite reported by Stendal (1990) could not be confirmed. However, to be of economic interest the mineralisation should have ≥2 wt.% REO (T. Vrålstad personal communication). The detected concentrations are far below the economic concentrations and, thus, the investigated anomalies are not of economic interest. However, compared with the average REO+Y_2O_3 concentration of Ca-poor granites, which is 0.031 wt.% according to Turekian and Wedepohl (1961), the Tysfjord granite gneisses are up to 5 times enriched in REO+Y_2O_3. The strong REE enrichment of the Tysfjord granite gneisses is remarkable from a scientific point of view and it is not clear which processes caused the REE-enrichment in the granites. The major carriers of the REE are allanite (LREE), zircon (HREE), and apatite (LREE). Titanite is presumably also an important LREE carrier in the Sommerset and Hellemobotn granite gneiss. Average grain sizes are 60 µm for allanite, 40 µm for zircon, 60 µm for apatite, and 200 µm for titanite. In addition two important findings were made. Firstly, granite gneiss with high-gamma-ray signals is not necessarily enriched in REE (Fig. 49) and secondly, fluids which are responsible for the U-mineralisation in the Sommerset granite gneiss leached REE from the rock.

This is a reconnaissance study that showed that the Tysfjord granite gneiss is the most REE-Zr-enriched basement area in central and northern Nordland. The REE-Zr enrichment is the cause for the high gamma-ray signal and the enrichment of REE-Zr in stream sediments

(Müller 2010). Because of the limited time in the field and difficult accessibility the areas of the most significant gamma-ray anomalies in the central and northern Tysfjord window between Reinoksvatn and Hellemobotn were not investigated (Fig. 50). The anomalies are aligned and bordered by large-scale NW-NNW-striking structures. The anomalies are presumably caused by TIB granite gneisses with enriched Th and REE. However, the $REO+Y_2O_3$ concentrations are presumably not higher than 0.5 wt.% based on the results of this report. However, strong local enrichments of $REO+Y_2O_3$ might occur within these anomalies which can be identified by ground survey with the scintillometer.

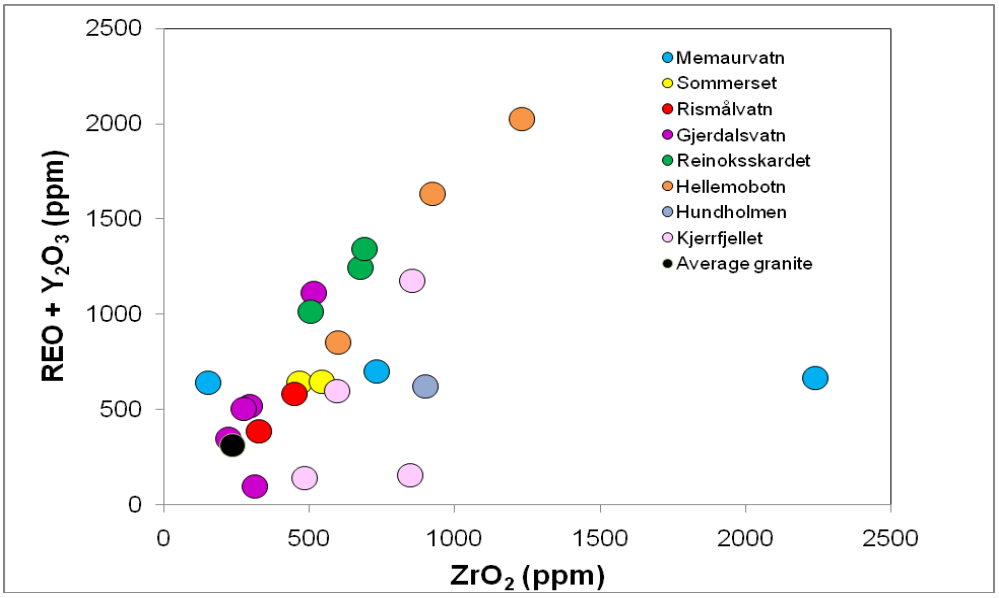

Figure 48. *Diagram of ZrO_2 versus $REO+Y_2O_3$ concentrations of TIB granite gneisses of the Rishaugfjellet, Sommerset and Tysfjord basement windows. The black dot represents the average composition of Ca-poor granites according to Turekian and Wedepohl (1961).*

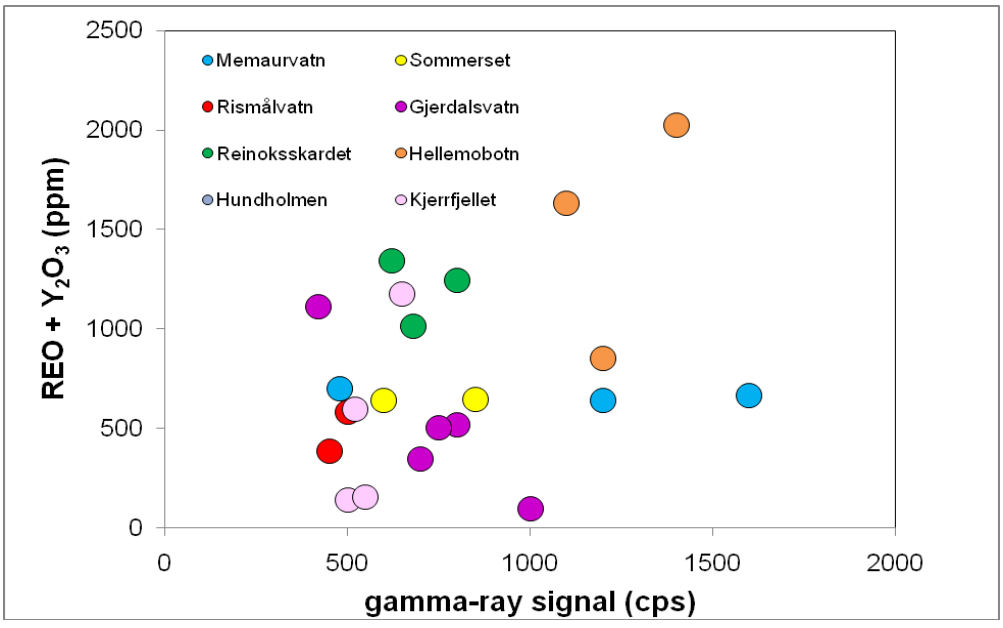

Figure 49. *Diagram of the gamma-ray signal measured with the scintillometer in the field plotted against the $REO+Y_2O_3$ concentration of TIB granite gneisses. Note that high gamma-ray signal does not necessarily indicate high $REO+Y_2O_3$ concentrations as is the case for the Memaurvatn samples.*

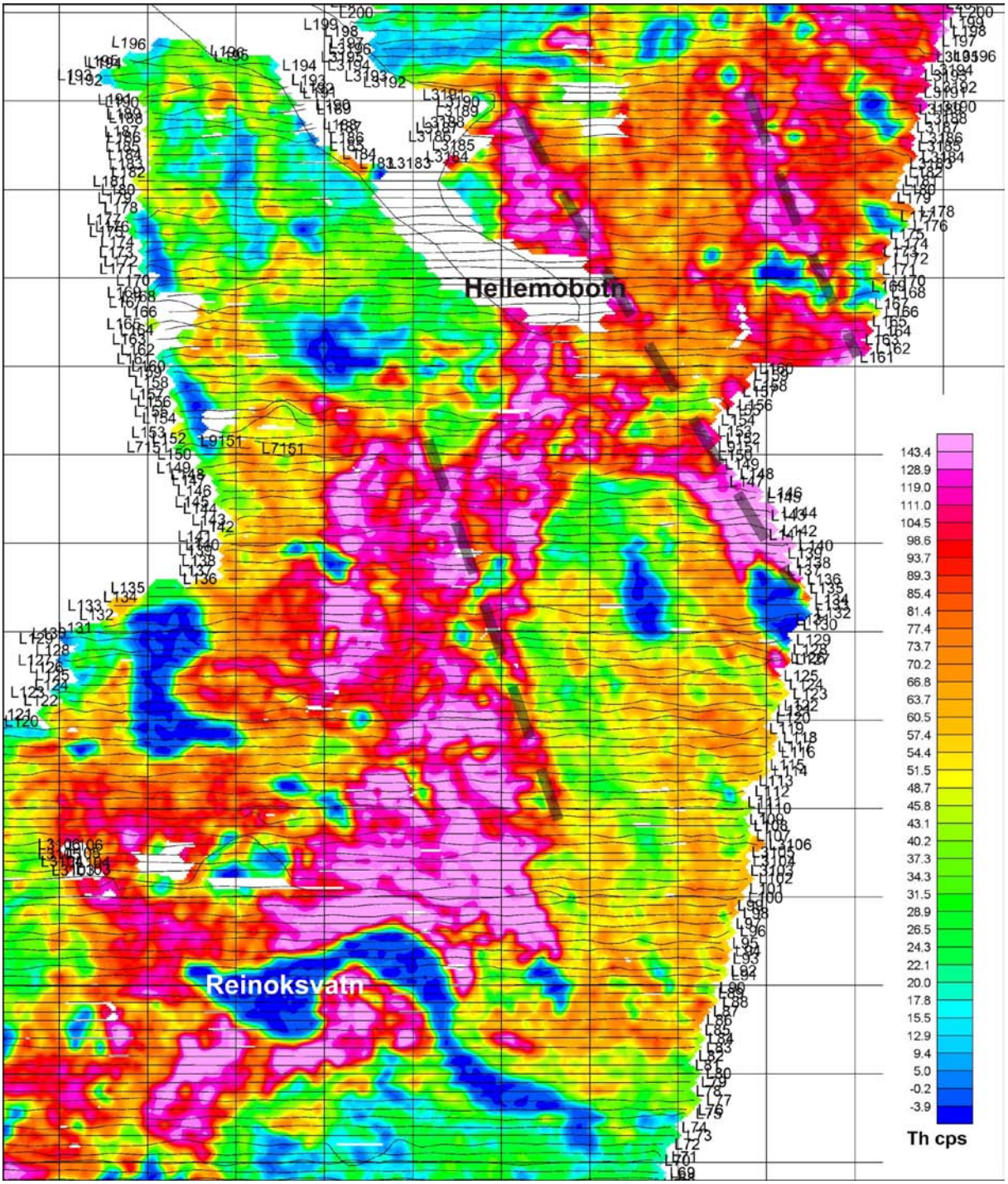

Figure 50. *Airborne-measured Th-radiation map of the Reinoksvatn-Hellemobotn area in the central eastern Tysfjord window obtained by NGU in 1991.*

8. References

Bea F. (1996) Residence of REE, Y, Th and U in granites and crustal protoliths; Implications for the chemistry of crustal melts. J. Petrol. 37:521-552.

Foslie S. (1941) Tysfjords geologi. Beskrivelse til det geologiske gradteigskart Tysfjord. NGU. 149, 298 p.

Gustavson M., Cooper M.A., Kollung S., Tragheim D.G. (2004) Geological Map of Fauske 2129 IV – 1 : 50 000. Geological Survey of Norway.

Hansen A.K. (1983) Undersøkelse af Mo-U-W mineraliseringer i Kalvikvinduet ved Sommerset, Sørfold, Nordland. NGU rapport 1900/30F.

Husdal T. (2008): The minerals of the pegmatites within the Tysfjord granite, northern Norway. Norsk Bergverksmuseum Skrift 38:5-28.

Müller A. (2010) Potential for rare earth element and Zr-, Be-, U-, Th-, (W-)mineralisations in central and northern Nordland. NGU report 2009.037.

Romer R.L., Kjøsnes B., Korneliussen A., Lindahl I., Skyseth T., Stendal M., Sundvoll B., (1992) The Archaean-Proterozoic boundary beneath the Caledonides of northern Norway and Sweden: U-Pb, Rb-Sr and Nd isotope data from the Rombak-Tysfjord area. NGU report 91.225, 67 p.

Seifert W. (2005) REE-, Zr-, and Th-rich titanite and associated accessory minerals from a kersantite in the Frankenwald, Germany. Miner. Petrol. 84:129-146

Solli A., Nordgulen Ø. (2006) Bedrock map of Norway and the Caledonides in Sweden and Finland scale 1 : 2 000 000. Geological Survey of Norway.

Stendal H. (1990) Mineraliseringspotential af granitiske bjergarter I den sydlige del af Tysfjordvinduet, Nordland, Norge. Geolognytt 1/90:106-107.

Turekian K.K., Wedepohl K.H. (1961) Distribution of the elements in some major unites of the Earth's crust. Bull. Geol. Soc. Amer. 72:172-202.

Vogt T. (1922) Über Thalenit von Hundholmen. Vid.-Selsk. Skrifter I.M.-N. Kl. 1:19-47.

Appendix 1.

Sample list.

	rock		sample nr.	UTM	E/N	
Memaurvatn	coarse-grained biotite granite gneiss	non-mineralised	22091001	33V	528891	7472316
	coarse-grained biotite granite gneiss	mineralised	22091002	33V	529262	7472074
	coarse-grained biotite granite gneiss with fluorite	mineralised	22091003	33V	529191	7471937
Kalvik	fine-grained biotite granite	non-mineralised	22091004	33V	523659	7484142
Sommerset	coarse-grained biotite granite gneiss	non-mineralised	22091005	33V	526488	7490451
	coarse-grained biotite granite gneiss	non-mineralised	22091006	33V	526470	7490431
	coarse-grained biotite granite gneiss	non-mineralised	22091007	33V	527724	7491575
	coarse-grained biotite granite gneiss	mineralised	22091008	33V	527828	7491610
	coarse-grained biotite granite gneiss	mineralised	22091009	33V	527753	7491584
	40-cm pegmatite lens	mineralised	22091010	33V	527724	7491575
Rismålsvatn	coarse-grained granitic gneiss	non-mineralised	22091011	33V	526562	7484093
	coarse-grained granitic gneiss	non-mineralised	22091012	33V	526430	7483933
Gjerdalsvatn	fine-grained biotite granite gneiss	mineralised	23091001	33V	548097	7509249
	fine-grained biotite granite gneiss	mineralised	23091002	33V	548030	7509236
	coarse-grained biotite granite gneiss	non-mineralised	23091003	33V	548063	7509252
	fine-grained biotite granite gneiss	mineralised	23091004	33V	548162	7509248
	fine-grained biotite granite gneiss	mineralised	28091009	33V	547785	7509232
Reinoksskardet	coarse-grained biotite granite gneiss	mineralised	23091005	33V	553447	7508142
	coarse-grained biotite granite gneiss	non-mineralised	23091007	33V	553446	7508686
	coarse-grained biotite granite gneiss	non-mineralised	23091008	33V	553061	7508248
	coarse-grained biotite granite gneiss	non-mineralised	23091009	33V	553350	7507550
Lagmannsvik pegmatite	thorium-uranium mineralisation in K-feldspar	mineralised	23091015	33V	536594	7535942
Kjerrfjellet	medium-grained biotite granite gneiss	non-mineralised	24091001	33V	544145	7555005
	medium-grained biotite granite gneiss	non-mineralised	24091002	33V	544242	7555186
	medium-grained biotite granitic gneiss	non-mineralised	24091003	33V	544103	7555094
	medium-grained biotite-rich granite gneiss	non-mineralised	24091004	33V	543823	7554846
Hellemobotn	medium-grained biotite granite gneiss	mineralised	25091001	33V	566519	7520464
	medium-grained biotite-rich granite gneiss	mineralised	25091002	33V	566519	7520464
	medium-grained biotite granite gneiss	mineralised	25091003	33V	566560	7520281
	medium-grained biotite granite gneiss	non-mineralised	25091004	33V	565950	7519621
	fine-grained porphyritic biotite gneiss	non-mineralised	25091005	33V	565552	7519525
	medium-grained biotite granite gneiss	non-mineralised	25091006	33V	565312	7519485
	medium-grained biotite granite gneiss	non-mineralised	25091007	33V	565023	7519733
Hundholmen	yttrofluorite	mineralised	28091004	33V	552639	7559801
	coarse-grained biotite granite gneiss	non-mineralised	28091005	33V	553636	7558054

Appendix 2.

Whole rock analyses of major elements.

rock type	sample	SiO_2	Al_2O_3	Fe_2O_3	TiO_2	MgO	CaO	Na_2O	K_2O	MnO	P_2O_5	LOI	total
Memaurvatnet	22091001	72.06	13.23	3.39	0.34	0.41	0.8	3.37	5.72	0.05	0.05	0.4	99.82
	22091002	72.56	12.43	3.93	0.27	0.62	0.58	3.03	5.63	0.08	0.04	0.5	99.67
	22091003	74.6	12.72	1.66	0.1	0.11	0.75	3.39	5.94	0.02	0.02	0.6	99.93
Kalvik	22091004	71.68	13.53	3.23	0.48	0.54	0.97	2.9	5.58	0.07	0.07	0.8	99.86
Sommerset	22091005	71.83	13.94	2.03	0.24	0.25	1.25	4.27	5.15	0.07	0.02	0.8	99.88
	22091006	64.51	17.29	3.1	0.31	0.68	1.4	5.41	6.04	0.09	0.04	1	99.82
	22091007	73.87	13.8	1.1	0.21	0.14	0.53	3.42	6.19	0.02	0.02	0.6	99.91
	22091008	75.28	12.98	1.47	0.21	0.16	0.51	3.16	5.8	0.02	0.02	0.3	99.94
	22091009	75.43	12.79	1.51	0.19	0.21	0.55	2.97	5.7	0.03	0.02	0.5	99.92
	22091010	79.29	11.36	1.66	0.2	0.34	0.57	4.35	1.51	0.02	<0.01	0.7	99.97
Rismålsvatnet	22091011	75.71	11.71	2.33	0.14	0.15	0.73	3.65	4.64	0.03	0.01	0.8	99.89
	22091012	76.61	12.14	1.61	0.1	0.1	0.17	3.69	4.99	0.02	0.01	0.5	99.93
Gjerdalsvatnet	23091001	73.72	13.61	2.09	0.22	0.27	0.77	3.92	5.02	0.03	0.04	0.2	99.87
	23091002	74.09	13.48	1.86	0.19	0.21	0.77	3.65	5.27	0.04	0.04	0.3	99.89
	23091003	73.32	13.08	2.49	0.23	0.08	0.77	3.34	6.01	0.05	0.03	0.4	99.78
	23091004	74.54	13.44	1.6	0.16	0.22	0.72	3.96	4.93	0.03	0.03	0.3	99.92
	28091009	73.2	13.68	1.9	0.19	0.21	0.97	3.44	5.54	0.04	0.04	0.7	99.92
Reinoksvatnet	23091005	71	14.34	2.35	0.09	0.09	1.01	3.94	6.42	0.03	0.01	0.7	99.95
	23091007	72.52	13.03	2.99	0.25	0.07	1.06	3.53	5.71	0.06	0.04	0.5	99.77
	23091008	71.81	13.53	3.14	0.27	0.13	0.96	3.54	5.77	0.06	0.03	0.5	99.75
	23091009	73.51	13.08	2.49	0.23	0.1	0.96	3.54	5.55	0.05	0.02	0.3	99.82
Kjerrfjellet	24091001	71.01	14.09	3.58	0.44	0.5	1.08	3.96	4.76	0.08	0.08	0.3	99.88
	24091002	69.44	14.09	4.09	0.51	0.5	1.35	3.7	5.56	0.08	0.09	0.4	99.79
	24091003	69.08	14.43	4.13	0.53	0.51	1.03	3.84	5.58	0.07	0.12	0.5	99.82
	24091004	69.58	13.19	5.35	0.55	1.11	0.71	3.01	5.53	0.08	0.13	0.5	99.72
Hellemobotn	25091001	69.29	14.77	3.42	0.41	0.43	1.2	4.05	5.42	0.06	0.07	0.7	99.81
	25091002	69.39	13.51	4.92	0.55	0.65	1.47	3.84	4.33	0.09	0.1	0.8	99.69
	25091003	68.86	12.61	6.43	0.76	0.72	1.75	3.53	3.89	0.11	0.15	0.8	99.61
	25091004	71.82	14.58	2.26	0.24	0.32	0.88	4.12	5.27	0.04	0.04	0.3	99.86
	25091005	70.92	14.05	2.78	0.37	0.37	1.28	3.66	5.51	0.04	0.08	0.8	99.82
	25091006	76.12	12.56	1.44	0.15	0.24	0.48	3.65	4.77	0.02	0.03	0.5	99.94
	25091007	74.97	12.7	1.81	0.18	0.17	0.8	3.52	5.3	0.04	0.04	0.4	99.93
Hundholmen	28091005	67.35	14.48	4.89	0.48	0.28	2.01	3.44	5.89	0.1	0.1	0.7	99.71

Appendix 3. Whole rock analyses of trace elements. REO – sum of all REO including Y_2O_3.

rock type	sample	Ba	Be	Co	Cs	Ga	Hf	Nb	Rb	Sn	Sr	Th	U	V	W	Zr	Mo	Cu	Pb	Zn	Ni	As	Cd
Memaurvatnet	22091001	405	8	1.4	3.5	24.8	15.8	33.7	286.1	6	75.9	41.1	12.7	<8	0.9	541.1	0.2	1.9	7.2	67	0.6	6.1	<0.1
	22091002	279	8	1.7	4.7	23.7	29.9	28.8	292.7	6	58.8	35.1	134.5	<8	0.8	1657.5	0.3	2.1	13.2	89	3.9	4	0.4
	22091003	137	8	0.6	2.9	24.6	4.5	18.8	314.3	3	31.2	61.5	10.1	<8	1.3	112.9	4.5	6.1	21.7	37	0.7	10	<0.1
Kalvik	22091004	706	2	3.6	2.9	17.4	7.5	15.2	185	1	167.8	10.3	3.6	24	<0.5	283.9	<0.1	3.9	2.9	63	3.9	0.5	<0.1
Sommerset	22091005	209	5	0.9	1.5	17.9	10.9	25.9	193.5	3	121.1	40.5	9.4	<8	<0.5	345.5	0.3	0.9	11.2	36	2.6	1.5	0.1
	22091006	224	11	2.4	3.5	27.3	14.4	37.8	288.3	4	101.7	42.5	27.7	<8	0.5	402.9	0.6	45.7	9.5	109	2	1.8	<0.1
	22091007	300	3	0.6	1.6	18.3	8.4	24.1	228.8	1	66.5	24	27.1	<8	<0.5	245.5	4.2	3.9	2.7	21	1.7	0.8	<0.1
	22091008	294	4	0.2	2.2	18.1	7.7	20.4	227.4	2	72.5	23.4	6.6	<8	<0.5	238.6	0.5	3	1.4	24	0.3	<0.5	<0.1
	22091009	272	4	1.1	2.3	18.4	8.7	22.6	222	<1	63.4	28.5	11.7	<8	<0.5	254.8	7.2	6.8	2.3	25	1.9	0.8	<0.1
	22091010	69	7	1.6	1.7	18.9	2.3	17.2	89.2	<1	53.6	4.4	120.9	16	1.4	54.5	79.1	1.9	4.4	23	3.2	14.1	<0.1
Rismålsvatnet	22091011	23	5	<0.2	1.2	32.5	14.3	57.4	305.8	7	7	21.5	7.6	<8	0.7	332.3	0.2	0.4	6.9	82	0.2	0.7	<0.1
	22091012	43	6	0.4	1.6	37	11.8	94.9	374.4	8	9.1	17.9	12.7	<8	0.9	242.4	0.7	7.5	14.4	78	0.4	1.1	<0.1
Gjerdalsvatnet	23091001	357	5	1	1.9	20.4	6.5	24.1	241.8	2	86.9	56.1	21.6	<8	<0.5	218.4	1.8	0.2	6.1	74	0.8	0.7	<0.1
	23091002	341	4	1.3	2.6	20.3	6.9	22	266.1	2	87	41.9	13.9	<8	<0.5	203.1	2.4	0.2	7.5	59	0.4	0.9	<0.1
	23091003	439	3	0.9	0.8	24.1	10.6	31.4	233.5	1	79.9	30.3	4.6	<8	<0.5	382.2	2	1	10.1	72	<0.1	1.3	<0.1
	23091004	261	4	1.2	2.4	19.8	5.9	22.5	243.1	<1	78.1	44	10.1	<8	<0.5	164.1	0.4	0.3	7.5	53	0.5	0.7	<0.1
	28091009	388	3	1.4	1.2	18.6	7.1	19.1	224.2	2	113.8	37.6	4.9	<8	<0.5	230.1	2.2	0.2	3	38	0.2	<0.5	<0.1
Reinoksvatnet	23091005	140	8	0.9	4	33.4	2.7	52.1	485.6	6	29.2	28.8	25.9	<8	1.4	36.7	0.6	2.1	7.4	83	<0.1	1	<0.1
	23091007	303	8	0.5	3.3	27.6	16	46.7	305	4	54.4	40.6	10.2	<8	0.6	499	1.4	0.4	12.8	127	1	1.7	<0.1
	23091008	308	6	1.2	2.7	27.1	15.4	48.2	277.9	4	67.1	39.2	8.9	<8	0.6	509.2	4.8	0.5	10.1	128	0.5	1.8	<0.1
	23091009	239	7	0.5	3	27.3	12.7	40.1	301.6	5	49.4	31.8	8.6	<8	0.6	374.3	0.9	0.5	9	112	0.2	1.2	<0.1
Kjerrfjellet	24091001	518	4	2.3	1.1	21.5	9.4	26.4	184.5	3	102.1	14.4	3.2	12	<0.5	357.2	1.7	2	2.7	64	0.4	0.9	<0.1
	24091002	625	5	2.7	1.5	22.5	11.7	32.1	228.8	4	117	39.9	7	14	<0.5	441.1	1.7	1.3	5.5	77	0.4	1.6	<0.1
	24091003	576	5	2.7	1.6	23.1	17.6	36.3	228.9	4	106.7	30.5	3.9	12	<0.5	626.4	0.3	2.8	5.1	80	0.6	1.4	<0.1
	24091004	522	7	2.8	2	22.3	15.6	32.6	262	3	95.6	17.6	7.7	15	<0.5	631.8	2.5	<0.1	6.8	101	0.7	1.5	<0.1
Hellemobotn	25091001	246	7	2.6	3.1	25.2	12.4	30.2	292.5	4	80.6	90.8	20.2	8	<0.5	443.2	0.7	<0.1	9.3	86	0.3	0.5	<0.1
	25091002	190	6	3.7	3.1	26.2	18.7	42.1	261.4	5	78.3	121.8	29.3	12	0.5	684	1.5	0.4	10.5	103	0.5	1.5	<0.1
	25091003	166	7	4.9	4.8	27.2	26.3	59.9	299.1	8	63	137.7	33.4	16	<0.5	909.9	1.6	0.4	10.2	143	1.2	1.5	<0.1
	25091004	229	5	1.5	2.3	22.2	10.3	21.6	288.4	2	70	70	17.6	<8	0.6	311.2	3.2	0.2	7.3	51	0.3	0.7	<0.1
	25091005	756	4	2.5	1.3	21	10	19.4	229.9	2	154	23.1	3.8	21	<0.5	383.1	2.6	1.1	3.6	43	1.3	0.5	<0.1
	25091006	137	5	3.3	0.9	21.5	7.4	23.5	270	4	89.7	62.6	13.6	<8	0.9	185.3	<0.1	0.4	4.3	15	0.9	<0.5	<0.1
	25091007	186	5	0.8	1.3	20.8	7.3	22.4	303.5	3	48.7	58.2	15.8	<8	<0.5	209.6	0.1	2.5	7.7	27	0.3	<0.5	<0.1
Hundholmen	28091005	1047	6	1.6	3.2	26	18.1	41.8	251.4	6	173.3	21.4	7.1	<8	1	665	2.7	2.6	9.5	111	0.4	2.2	0.1

Appendix 3. Continued.

rock type	sample	Sb	Bi	Au	Hg	Tl	Se	Y	La	Ce	Pr	Nd	Sm	Eu	Gd	Tb	Dy	Ho	Er	Tm	Yb	Lu	REO
Memaurvatnet	22091001	0.5	0.1	<0.5	<0.01	0.6	1.2	65.1	107.4	241.8	25.99	94.5	15.81	1	12.02	2.11	12.01	2.39	6.61	0.97	6.47	0.96	702.10
	22091002	0.3	0.2	<0.5	<0.01	0.8	2.2	158.3	74.2	161.4	17.32	60.3	14.76	0.82	17.34	2.94	18.95	4.3	13.05	1.79	11.04	1.59	667.28
	22091003	0.7	0.1	<0.5	<0.01	0.4	1.2	30.7	125.4	268	22.52	70.5	9.34	0.44	4.96	0.9	4.89	0.96	2.92	0.46	3.36	0.53	641.85
Kalvik	22091004	<0.1	<0.1	<0.5	<0.01	0.6	<0.5	17.4	28.5	57.4	6.69	24.6	4.23	0.68	3.03	0.52	2.96	0.64	1.89	0.32	2.32	0.36	178.81
Sommerset	22091005	<0.1	0.1	<0.5	<0.01	0.3	1	43.7	112.3	243.1	23.88	80.2	12.12	0.5	7.65	1.38	7.82	1.6	4.75	0.73	5.06	0.78	642.38
	22091006	0.1	<0.1	<0.5	<0.01	0.7	1.2	39.4	112.3	243.2	25.16	88.2	12.84	0.52	9.29	1.38	7.12	1.32	3.98	0.63	4.08	0.7	647.29
	22091007	<0.1	<0.1	0.6	<0.01	0.3	0.7	46.2	55.7	104	13.48	47.6	7.46	0.5	5.37	1.04	6.65	1.58	5.1	0.9	6.23	0.92	358.23
	22091008	<0.1	<0.1	1.3	<0.01	0.3	<0.5	14.1	5.1	12.5	1.13	4	0.84	0.27	1.03	0.24	1.85	0.48	1.64	0.28	1.94	0.33	54.73
	22091009	<0.1	<0.1	<0.5	<0.01	0.3	<0.5	27.2	22.9	131.1	5.68	19.6	3.32	0.3	2.86	0.57	3.74	0.96	3.25	0.57	3.8	0.61	267.55
	22091010	<0.1	<0.1	<0.5	<0.01	0.3	<0.5	7.6	6	11.8	1.09	3.3	0.62	0.18	0.8	0.18	1.02	0.27	0.81	0.13	0.86	0.14	41.39
Rismålsvatnet	22091011	<0.1	<0.1	<0.5	<0.01	0.6	<0.5	86.2	109.7	226.9	22.69	76.7	13.79	0.54	11.54	2.1	12.02	2.62	8.05	1.28	8.45	1.23	690.89
	22091012	<0.1	<0.1	<0.5	<0.01	0.6	<0.5	67.6	66.8	142.9	13.41	44.2	8.59	0.35	7.51	1.67	11.06	2.42	7.96	1.23	7.9	1.17	456.17
Gjerdalsvatnet	23091001	<0.1	<0.1	<0.5	<0.01	0.6	<0.5	31.9	95.6	197.6	19.27	63.7	9.45	0.61	6.63	1.04	5.72	1.1	3.05	0.48	2.97	0.4	517.28
	23091002	<0.1	<0.1	<0.5	<0.01	0.6	<0.5	34.7	94.5	184.7	19.04	61.9	9.35	0.62	6.98	1.14	6.27	1.24	3.6	0.53	3.33	0.51	504.47
	23091003	<0.1	<0.1	<0.5	<0.01	0.4	<0.5	53.3	198.7	444	42.56	148.2	20.03	1.27	13.61	2.03	10.06	1.9	5.51	0.8	4.86	0.75	1113.84
	23091004	<0.1	<0.1	<0.5	<0.01	0.6	<0.5	24.4	62.1	127.6	13.34	44.5	6.75	0.48	5.27	0.85	4.5	0.91	2.49	0.37	2.29	0.32	348.77
	28091009	<0.1	<0.1	<0.5	<0.01	0.4	<0.5	19	7.9	33	1.99	6.8	1.91	0.23	1.81	0.42	2.84	0.66	2.07	0.31	2.19	0.31	96.98
Reinoksvatnet	23091005	<0.1	<0.1	<0.5	<0.01	1	<0.5	75.8	8.7	32.9	4.87	25.8	9.7	0.52	10.03	1.97	12.68	2.76	8.9	1.38	9	1.25	247.64
	23091007	<0.1	<0.1	<0.5	<0.01	0.8	<0.5	90.6	210.9	461.2	46.65	160.1	24.54	1.06	18.41	2.92	16.38	3.04	9.03	1.32	8.34	1.22	1243.56
	23091008	<0.1	<0.1	<0.5	<0.01	0.7	<0.5	96.3	229.1	501.2	50.17	173.8	25.84	1.02	18.93	3.02	16.71	3.29	9.37	1.37	8.83	1.26	1343.01
	23091009	<0.1	<0.1	<0.5	<0.01	0.8	<0.5	83	177.8	370	37.1	123.6	19.36	0.77	13.69	2.29	13.11	2.55	7.54	1.16	7.7	1.07	1014.82
Kjerrfjellet	24091001	<0.1	<0.1	<0.5	<0.01	0.6	<0.5	34.2	9.5	29.4	3.41	15.1	3.84	0.41	3.53	0.72	4.59	1.16	4.11	0.68	4.94	0.83	139.11
	24091002	<0.1	<0.1	<0.5	<0.01	0.6	<0.5	53.7	102.8	218.1	19.75	65	10.96	1.07	8.85	1.5	8.86	1.82	5.28	0.82	5.51	0.83	595.63
	24091003	<0.1	<0.1	<0.5	<0.01	0.7	<0.5	43	7.5	25.8	3.72	17.2	5.18	0.52	5.52	1.06	6.69	1.41	4.44	0.72	4.88	0.73	153.84
	24091004	<0.1	<0.1	<0.5	<0.01	1	0.5	94.5	186.6	411.4	44.91	163.3	27.04	2.07	22.58	3.49	19.08	3.68	10.35	1.44	8.39	1.17	1178.35
Hellemobotn	25091001	<0.1	<0.1	<0.5	<0.01	0.9	<0.5	51	161.1	332.5	31.21	99.3	14.58	0.6	9.83	1.58	9.25	1.68	5.05	0.76	5.14	0.77	852.42
	25091002	<0.1	<0.1	<0.5	<0.01	1	<0.5	93.1	322.5	640.5	58.08	189	25.68	0.77	18.17	2.82	15.77	2.97	8.6	1.29	8.32	1.26	1634.12
	25091003	<0.1	<0.1	<0.5	<0.01	1.5	<0.5	117.5	398.8	791.4	72.96	233.2	31.88	0.76	22.5	3.64	19.83	3.89	11.48	1.75	11.34	1.72	2027.02
	25091004	<0.1	<0.1	<0.5	<0.01	0.8	<0.5	38.3	121.6	259	24.58	80.1	12.01	0.62	7.75	1.24	6.71	1.22	3.64	0.55	3.54	0.52	660.52
	25091005	<0.1	<0.1	<0.5	<0.01	0.5	<0.5	24.2	69.1	161.7	15.52	52	8.03	0.8	5.5	0.84	4.4	0.82	2.28	0.33	2.12	0.32	409.42
	25091006	<0.1	0.1	<0.5	<0.01	0.3	<0.5	29.3	26.9	71.7	6.03	19.5	3.34	0.2	2.62	0.57	3.75	0.89	2.93	0.49	3.21	0.47	203.81
	25091007	<0.1	<0.1	<0.5	<0.01	0.4	<0.5	36.7	60.8	133	12.54	40.9	6.89	0.33	5.44	0.95	5.57	1.13	3.55	0.59	4.04	0.62	369.64
Hundholmen	28091005	0.1	0.1	<0.5	<0.01	0.7	<0.5	86.7	75.9	186.4	21.34	82.7	15.83	1.95	13.18	2.33	13.71	2.83	8.54	1.35	9.4	1.47	620.19